ODN-lipoplex (data not shown). The levels of TNF-α or IL-12 (p70) reached a peak at 12 or 6 h after intraperitoneal injection of CpG ODN-lipoplex, respectively. (TNF-α 155±43 pg/ml, IL-12 (p70) 292±79 pg/ml). On the other hand, GpC ODN-lipoplex induced less TNF-α and IL-12 (p70) secretion in the peritoneal cavity. (Fig. 4)

3.4. Administration route-dependent antitumor activity of CpG ODN-lipoplex

To examine whether the antitumor effect of CpG ODN-lipoplex is induced by local or systemic immune activation, we evaluated the effect of the administration route of the CpG ODN-lipoplex on its antitumor activity. To this end, mice bearing peritoneal B16-BL6/Luc tumor cells were injected with CpG ODN-lipoplex via different administration routes.

Injection of CpG ODN-lipoplex into the tail vein or into the dorsal skin hardly reduced the number of tumor cells in the greater omentum (Fig. 5A). Fig. 5B shows TNF-α and IL-12 (p70) production in the peritoneal cavity after administration of CpG ODN-lipoplex via one of the different routes. In the peritoneal lavage of mice given intravenous or intradermal injections, the level of TNF-α was hardly changed (21±12 pg/ml, 36±4 pg/ml, respectively). As for IL-12 (p70), in mice given intravenous or intradermal injections, the level of production was below the limits of detection, which was in marked contrast to the results obtained with the intraperitoneal CpG ODN-lipoplex as mentioned above. These results suggest that the local immune response in the peritoneal cavity is essential for inhibition of the peritoneal dissemination of tumor cells by the CpG ODN-lipoplex.

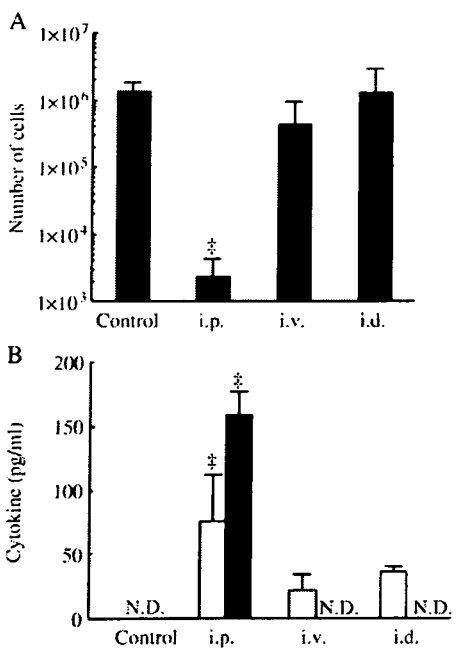

Fig. 5. Effect of the administration route of CpG ODN-lipoplex. (A) The number of B16-BL6/Luc cells in the greater omentum of mice, and (B) TNF-α and IL-12 (p70) in peritoneal lavage. B16-BL6/Luc tumor cells were given to C57BL/6 mice by intraperitoneal injection. CpG ODN-lipoplex was administered intraperitoneally, intravenously, or intradermally following tumor inoculation. (A) After 7 days, mice were sacrificed and the luciferase activity of the greater omentum was measured. ‡ $p<0.01$; The number of cells was significantly different from control group (t-test). (B) Six hours later, peritoneal lavage was collected and the levels of TNF-α (open bar) and IL-12 (p70) (closed bar) were measured by ELISA. Results are expressed as the mean+SD of at least 4 mice. These experiments shown are representative of two experiments with similar results. N.D.: not detected (TNF-α<16 pg/ml, IL-12 (p70)<62 pg/ml).

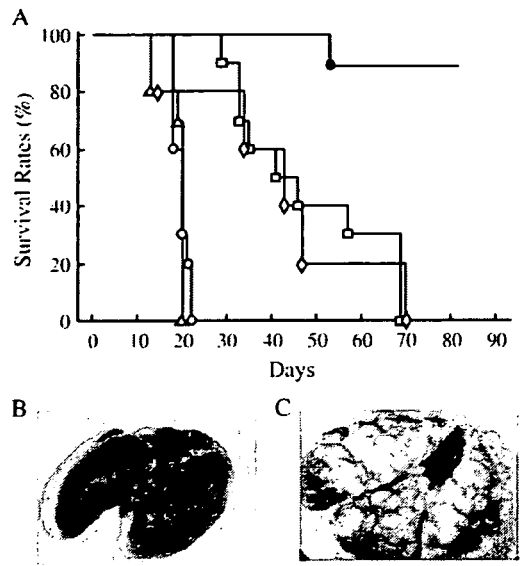

Fig. 6. (A) Survival rate of colon26/Luc tumor-bearing mice. On day 0, CDF1 mice were intraperitoneally inoculated with colon26/Luc cells. Tumor-bearing mice were treated with saline (○), cationic liposomes (□), naked CpG ODN (△), random ODN-lipoplex (◇), or CpG ODN-lipoplex (●). (B, C) Representative lung colonies after intravenous injection of colon26/Luc cells. The survival of the CpG ODN-lipoplex was significantly longer than the groups given saline, cationic liposomes, naked CpG ODN, or random ODN-lipoplex ($p<0.0001$). (B) Long-time survivors; i.e., CDF1 mice that failed to establish peritoneal dissemination after primary and secondary challenge with colon26/Luc cells (these mice received CpG ODN-lipoplex soon after tumor inoculation) were rechallenged intravenously with colon26/Luc cells. At day 200 after the first challenge, all surviving mice were sacrificed. (C) Control mice were injected intravenously with colon26/Luc cells. After 20 days, mice were sacrificed. The experiment shown is representative of two experiments with similar results.

3.5. Prolongation of survival time of colon26/Luc-bearing mice by CpG ODN-lipoplex

Fig. 6A shows the survival rate of CDF1 mice after inoculation with colon26/Luc cells in the peritoneal cavity, followed by the intraperitoneal injection of saline, cationic liposomes, naked CpG ODN, CpG ODN-lipoplex, or random ODN-lipoplex. The saline or CpG ODN-treated groups all died by day 20. Cationic liposomes or random ODN-lipoplex slightly increased the survival time. However, about 90% of the CpG ODN-lipoplex-treated mice survived more than 80 days.

To examine whether the surviving mice acquired immunity to colon26/Luc cells, they were again given intraperitoneal injections of the tumor cells without any additional CpG ODN-lipoplex. Table 1 summarizes the survival time in mice rechallenged with these tumor cells. Although 2 out of 8 mice

Table 1
Immunological memory in surviving mice

	1st i.p.	2nd i.p. (on day 80)	i.v. (on day 144)
Saline	0/10		
CpG ODN-lipoplex	8/9	6/8	4/6

Long-term survivors of mice treated with CpG ODN-lipoplex in the survival experiment were rechallenged with colon26/Luc cells intraperitoneally on day 80 and intravenously on day 140 after the first inoculation of tumor cells.

died within 60 days after the second inoculation of the tumor cells, other mice survived more than an additional 60 days, suggesting that the tumor cells are rejected in these individuals. Then, the surviving mice were given injections of colon26/Luc cells into the tail vein, without the administration of CpG ODN-lipoplex. Again, 4 out of 6 mice were alive for more than an additional 60 days after the intravenous inoculation. At day 200 after the initial inoculation, all surviving mice were sacrificed. The lungs of mice surviving long-term had no visible tumor colonies on the lung surface (Fig. 6B) and no detectable luciferase activity. In a quite contrast, an injection of colon26/Luc cells into the tail vein of naïve mice resulted in the formation of a number of tumor colonies in the lung (Fig. 6C).

4. Discussion

Generally speaking, during the initial stages of peritoneal dissemination, tumor cells in the peritoneal cavity selectively infiltrate into the milky spots of the greater omentum, which is the primitive lymphoid tissue in the peritoneal cavity [22]. Tumor cells present in milky spots finally form an omental cake, so the proliferation of tumor cells in the greater omentum is a life-threatening event in peritoneal dissemination patients [21]. In this study, we found that PO-type CpG oligonucleotides complexed with cationic liposomes effectively inhibit the tumor growth in the greater omentum in the mouse model of peritoneal dissemination.

Previous studies demonstrated that oligonucleotide containing CpG motifs is a very strong activator of monocytes, macrophages, B cells, and DCs [23]. The CpG motif that appears to be optimal for stimulating murine immune cells is different from that for human cells. CpG dinucleotide flanked by two purine bases on the 5′-side and two pyrimidine bases on the 3′ side, such as GACGTT, efficiently activates the murine immune system, whereas the optimal motif for humans is GTCGTT. In addition, it has been reported that the biological activity of a given hexamer is strongly modulated by the remaining sequences within the ODN. For example, in mice, the immune stimulatory effects of CpG ODN were enhanced if the ODN had a TpC dinucleotide on the 5′ end and was pyrimidine-rich on the 3′ side. In addition, ODN with two or three CpG motifs in the sequence were found to be very potent compared to those with only one CpG motif [23]. The CpG motifs in ODN containing several motifs should not be back-to-back but preferably have at least two intervening bases, preferably Ts [3,9]. Moreover, single-stranded CpG ODN can stimulate immune functions more strongly than the double-stranded counterpart [24]. Therefore, in this study, based on these previous findings, we designed a single-stranded CpG ODN with the sequence 5′-TCGACGTTTTGACGTTTTGACGTTTT-3′ to induce effective immune responses, and found that the ODN can induce enough antitumor activity in mice when administered as a lipoplex. The importance of the sequence on the ODN-mediated antitumor activity was examined by using GpC ODN-lipoplex. Then we found that GpC ODN-lipoplex induced little TNF-α production from RAW264.7 cells. These results strongly suggest that TLR-9, the receptor recognizing the CpG motif, is involved in the antitumor activity of CpG ODN-lipoplex.

Oligonucleotide with the normal phosphodiester (PO) backbone is rapidly degraded by nucleases in serum and intracellular compartments. Phosphorothioate (PS) modification has been commonly used to stabilize oligonucleotides, but it has also been suggested that PS-type CpG ODN induces systemic toxicity, such as a transient anticoagulant effect, activation of complement cascade, and inhibition of basic fibroblast growth factor binding to surface receptors, because of non-specific protein binding [12,13]. In this study, instead of using PS-type CpG ODN, we used a PO-type CpG ODN complex with cationic liposomes to stabilize against degradation.

Cationic liposomes have been investigated for the stabilization of nucleic acids against degradation [15]. Indeed, cationic liposome-based gene delivery vectors are known for their ability to protect pDNA from serum nuclease degradation [25]. This feature allows PS modification to be avoided. There is another advantage of using CpG ODN and a cationic liposome complex. Lipoplex is recognized as a foreign material, and is phagocytosed by immune cells, especially by mononuclear phagocytes. These cells express TLR-9, and recognize CpG motifs in DNA via the receptors and produce Th-1 type cytokines, which are a form of cancer immunotherapy [15,26–28]. Indeed, in this study, mouse macrophage-like RAW264.7 cells stimulated with CpG ODN-lipoplex induced a large amount of TNF-α while naked CpG ODN resulted in only a minor degree of induction. Therefore, it is suggested that the formation of a cationic liposome complex can deliver CpG ODN more effectively to macrophages than naked CpG ODN. Moreover, intraperitoneal injection of CpG ODN-lipoplex can induce Th-1 type cytokines such as TNF-α and IL-12 (p70) in ascitic fluid. Therefore, CpG ODN is delivered to peritoneal immunocompetent cells, such as macrophages, where CpG motifs are recognized and these results in the production of several Th-1 type cytokines. The cytokine levels detected after administration of CpG ODN-lipoplex to mice were much lower than those detected after addition to RAW264.7 cells. This discrepancy could be explained by the distribution and elimination of cytokines in vivo, and by the higher reactivity of RAW264.7 cells to CpG DNA than peritoneal macrophages [29].

There are many phagocytic cells in the body that express TLR-9, for example, DCs, peritoneal macrophages, Kupffer cells, splenic macrophages, and Langerhans' cells. When injected intraperitoneally, intravenously, or intradermally, CpG ODN-lipoplex is thought to be mainly recognized by peritoneal macrophages, Kupffer cells and splenic macrophages, or Langerhans' cells, respectively. Previous studies demonstrated

that intravenous or intradermal injection of CpG DNA induces systemic immune responses [16,30]. In the present study, we also found that an intravenous administration of CpG ODN-lipoplex significantly increased the serum concentration of TNF-α (data not shown). However, no significant changes were observed in the cytokine levels in the peritoneal cavity after injection of the lipoplex into the tail vein or into the dorsal skin. Thus, it is suggested that the local immunostimulation produced by CpG ODN-lipoplex in the peritoneal cavity is important for the inhibition of the peritoneal dissemination of tumor cells. It appears that immunocompetent cells in the peritoneal cavity are efficiently activated by intraperitoneal injection of CpG ODN-lipoplex and then induce a localized immune response.

Intraperitoneal administration of CpG ODN-lipoplex prolonged the survival of the peritoneal dissemination mice. Surviving mice persisted in spite of second inoculation of tumor cells into the peritoneal cavity. Furthermore, no visible tumor colonies were detected in the lung of the surviving mice that received an intravenous injection of colon26/Luc cells, whereas all naïve mice produced a number of metastatic colonies in the lung by the injection. So it appears that CpG ODN-lipoplex induces systemic and long-lasting antitumor activity. Further studies are needed to clarify the long-lasting antitumor mechanisms of CpG ODN-lipoplex.

In conclusion, a single administration of PO-type CpG ODN/cationic liposome complex can induce Th-1 type cytokines in the peritoneal cavity, and inhibit peritoneal dissemination in mice. Local immune activation in the peritoneal cavity is found to be important for the inhibition of peritoneal dissemination, because intraperitoneal injection of CpG ODN-lipoplex was more effective in reducing peritoneal tumor cells than intravenous or intradermal injection of CpG ODN-lipoplex. Moreover, the immune responses induced by CpG ODN-lipoplex can be effective in preventing tumor growth in and outside the peritoneal cavity. Immunotherapy with CpG ODN-lipoplex is not limited by the type of tumor cells. Therefore, CpG ODN-lipoplex is a potentially useful tool for the treatment of a broad range of tumor types.

Acknowledgements

This work was supported in part by grants from the Ministry of Health, Labour and Welfare, Japan.

References

[1] S. Gurunathan, D.M. Klinman, R.A. Seder, DNA vaccines: immunology, application, and optimization, Annu. Rev. Immunol. 18 (2000) 927–974.
[2] T. Tokunaga, H. Yamamoto, S. Shimada, H. Abe, T. Fukuda, Y. Fujisawa, Y. Furutani, O. Yano, T. Kataoka, T. Sudo, N. Makiguchi, T. Suganuma, Antitumor activity of deoxyribonucleic acid fraction from *Mycobacterium bovis* BCG, J. Natl. Cancer Inst. 72 (1984) 955–962.
[3] A.M. Krieg, A.K. Yi, S. Matson, T.J. Waldschmidt, A. Bishop, R. Teasdale, G.A. Koretzky, D.M. Klinman, CpG motifs in bacterial DNA trigger direct B-cell activation, Nature 374 (1995) 546–549.
[4] H. Hemmi, O. Takeuchi, T. Kawai, T. Kaisho, S. Sato, H. Sanjo, M. Matsumoto, K. Hoshino, H. Wagner, K. Takeda, S. Akira, A Toll-like receptor recognizes bacterial DNA, Nature 408 (2000) 740–745.
[5] A.K. Yi, J.H. Chace, J.S. Cowdery, A.M. Krieg, IFN-gamma promotes IL-6 and IgM secretion in response to CpG motifs in bacterial DNA and oligodeoxynucleotides, J. Immunol. 156 (1996) 558–564.
[6] D.M. Klinman, A.K. Yi, S.L. Beaucage, J. Conover, A.M. Krieg, CpG motifs present in bacteria DNA rapidly induce lymphocytes to secrete interleukin 6, interleukin 12, and interferon gamma, Proc. Natl. Acad. Sci. U. S. A. 93 (1996) 2879–2883.
[7] Z.K. Ballas, W.L. Rasmussen, A.M. Krieg, Induction of NK activity in murine and human cells by CpG motifs in oligodeoxynucleotides and bacterial DNA, J. Immunol. 157 (1996) 1840–1845.
[8] G.B. Lipford, M. Bauer, C. Blank, R. Reiter, H. Wagner, K. Heeg, CpG-containing synthetic oligonucleotides promote B and cytotoxic T cell responses to protein antigen: a new class of vaccine adjuvants, Eur. J. Immunol. 27 (1997) 2340–2344.
[9] A.K. Yi, M. Chang, D.W. Peckham, A.M. Krieg, R.F. Ashman, CpG oligodeoxyribonucleotides rescue mature spleen B cells from spontaneous apoptosis and promote cell cycle entry, J. Immunol. 160 (1998) 5898–5906.
[10] R. Rankin, R. Pontarollo, X. Ioannou, A.M. Krieg, R. Hecker, L.A. Babiuk, S. van Drunen Littel-van den Hurk, CpG motif identification for veterinary and laboratory species demonstrates that sequence recognition is highly conserved, Antisense Nucleic Acid Drug Dev. 11 (2001) 333–340.
[11] Q. Zhao, J. Temsamani, R.Z. Zhou, S. Agrawal, Pattern and kinetics of cytokine production following administration of phosphorothioate oligonucleotides in mice, Antisense Nucleic Acid Drug Dev. 7 (1997) 495–502.
[12] S.M. Fennewald, R.F. Rando, Inhibition of high affinity basic fibroblast growth factor binding by oligonucleotides, J. Biol. Chem. 270 (1995) 21718–21721.
[13] S.P. Henry, P.C. Giclas, J. Leeds, M. Pangburn, C. Auletta, A.A. Levin, D.J. Kornbrust, Activation of the alternative pathway of complement by a phosphorothioate oligonucleotide: potential mechanism of action, J. Pharmacol. Exp. Ther. 281 (1997) b810–b816.
[14] M. Rutz, J. Metzger, T. Gellert, P. Luppa, G.B. Lipford, H. Wagner, S. Bauer, Toll-like receptor 9 binds single-stranded CpG-DNA in a sequence- and pH-dependent manner, Eur. J. Immunol. 34 (2004) 2541–2550.
[15] O. Zelphati, F.C. Szoka, Mechanism of oligonucleotide release from cationic liposomes, Proc. Natl. Acad. Sci. U. S. A. 93 (1996) 11493–11498.
[16] M.M. Whitmore, S. Li, L. Falo Jr., L. Huang, Systemic administration of LPD prepared with CpG oligonucleotides inhibits the growth of established pulmonary metastases by stimulating innate and acquired antitumor immune responses, Cancer Immunol. Immunother. 50 (2001) 503–514.
[17] K. Hyoudou, M. Nishikawa, Y. Umeyama, Y. Kobayashi, F. Yamashita, M. Hashida, Inhibition of metastatic tumor growth in mouse lung by repeated administration of polyethylene glycol-conjugated catalase: quantitative analysis with firefly luciferase-expressing melanoma cells, Clin. Cancer Res. 10 (2004) 7685–7691.
[18] G. Poste, J. Doll, I.R. Hart, I.J. Fidler, In vitro selection of murine B16 melanoma variants with enhanced tissue-invasive properties, Cancer Res. 40 (1980) 1636–1644.
[19] T.H. Corbett, D.P. Griswold Jr., B.J. Roberts, J.C. Peckham, F.M. Schabel Jr., Tumor induction relationships in development of transplantable cancers of the colon in mice for chemotherapy assays, with a note on carcinogen structure, Cancer Res. 35 (1975) 2434–2439.
[20] S. Fumoto, F. Nakadori, S. Kawakami, M. Nishikawa, F. Yamashita, M. Hashida, Analysis of hepatic disposition of galactosylated cationic liposome/plasmid DNA complexes in perfused rat liver, Pharm. Res. 20 (2003) 1452–1459.
[21] L.F. Krist, M. Kerremans, D.M. Brockhuis-Fluitsma, I.L. Eesternans, S. Meyer, R.H. Beelen, Milky spots in the greater omentum are predominant sites of local tumour cell proliferation and accumulation in the peritoneal cavity, Cancer Immunol. Immunother. 47 (1998) 205–212.
[22] H. Tsujimoto, T. Takhashi, A. Hagiwara, M. Shimotsuma, C. Sakakura, K. Osaki, S. Sasaki, M. Shirasu, T. Sakakibara, T. Ohyama, A. Sakuyama, M. Ohgaki, T. Imanishi, J. Yamasaki, Site-specific implantation in the milky spots of malignant cells in peritoneal dissemination: immunohistochemical observation in mice inoculated intraperitoneally with bromodeoxyuridine-labelled cells, Br. J. Cancer 71 (1995) 468–472.

[23] A.M. Krieg, CpG motifs in bacterial DNA and their immune effects, Annu. Rev. Immunol. 20 (2002) 709–760.
[24] S. Zelenay, F. Elias, J. Flo, Immunostimulatory effects of plasmid DNA and synthetic oligodeoxynucleotides, Eur. J. Immunol. 33 (2003) 1382–1392.
[25] P.L. Felgner, G.M. Ringold, Cationic liposome-mediated transfection, Nature 337 (1989) 387.
[26] G. Trinchieri, Interleukin-12: a cytokine produced by antigen-presenting cells with immunoregulatory functions in the generation of T-helper cells type 1 and cytotoxic lymphocytes, Blood 84 (1994) 4008–4027.
[27] M.T. Lotze, L. Zitvogel, R. Campbell, P.D. Robbins, E. Elder, C. Haluszczak, D. Martin, T.L. Whiteside, W.J. Storkus, H. Tahara, Cytokine gene therapy of cancer using interleukin-12: murine and clinical trials, Ann. N.Y. Acad. Sci. 795 (1996) 440–454.
[28] K. Yasuda, Y. Ogawa, M. Kishimoto, T. Takagi, M. Hashida, Y. Takakura, Plasmid DNA activates murine macrophages to induce inflammatory cytokines in a CpG motif-independent manner by complex formation with cationic liposomes, Biochem. Biophys. Res. Commun. 293 (2002) 344–348.
[29] K. Yasuda, H. Kawano, I. Yamane, Y. Ogawa, T. Yoshinaga, M. Nishikawa, Y. Takakura, Restricted cytokine production from mouse peritoneal macrophages in culture in spite of extensive uptake of plasmid DNA, Immunology 111 (2004) 282–290.
[30] L. Liu, X. Zhou, H. Liu, L. Xiang, Z. Yuan, CpG motif acts as a 'danger signal' and provides a T helper type 1-biased microenvironment for DNA vaccination, Immunology 115 (2005) 223–230.

COMMUNICATION TO THE EDITOR

Moment Analysis for Kinetics of Gene Silencing by RNA Interference

Yuki Takahashi,[1] Kiyoshi Yamaoka,[1] Makiya Nishikawa,[1] Yoshinobu Takakura[2]

[1]Graduate School of Pharmaceutical Sciences, Kyoto University, Kyoto, Japan
[2]Department of Biopharmaceutics and Drug Metabolism, Graduate School of Pharmaceutical Sciences, Kyoto University, Sakyo-ku, Kyoto 606-8501, Japan; telephone: +81-75-753-4615; fax: +81-753-4614; e-mail: takakura@pharm.kyoto-u.ac.jp

Received 21 June 2005; accepted 8 August 2005

Published online 29 September 2005 in Wiley InterScience (www.interscience.wiley.com). DOI: 10.1002/bit.20718

Abstract: RNA interference (RNAi) was quantitatively evaluated from a kinetic viewpoint. A simple kinetic evaluation based on moment analysis was proposed, assuming suppression and recovery phases of gene expression. We defined the area under the curve of the inhibitory effect (AUC_{IE}) as an index of the total intensity of RNAi and the mean response time of the inhibitory effect (MRT_{IE}) as an index of its duration. The proposed kinetic analysis helps to understand the RNAi effect in a quantitative and time-dependent manner, which will be beneficial for designing RNAi-based gene silencing for both experimental and therapeutic purposes.

Keywords: RNA interference; gene silencing; moment analysis; luciferase

INTRODUCTION

RNA interference (RNAi) is a post-transcriptional gene silencing event, in which short double-stranded RNA (small interfering RNA; siRNA) degrades a target mRNA with a specific complimentary sequence and eventually blocks the translation of the protein encoded (Tuschl et al., 1999; Zamore et al., 2000). Since the discovery that siRNA can induce RNAi in mammalian cells without a sequence-nonspecific response (Caplen et al., 2001; Elbashir et al., 2001), RNAi has been widely used as an experimental tool to suppress specific gene expression when analyzing the function of a gene. This is because RNAi is attractive in terms of speed, convenience, and lower cost, compared with conventional methods to suppress gene function, such as gene knock-out by homologous recombination (McManus and Sharp, 2002). In addition, RNAi is more powerful than antisense strategies as far as the reduction in mRNA expression is concerned (Miyagishi et al., 2003). Moreover, RNAi is expected to be used as a therapeutic tool in the future treatment of various diseases, such as cancer, viral infections, and neurodegenerative disorders (Milhavet et al., 2003). In order to effectively use siRNA-based gene silencing as both an experimental and therapeutic tool, the intensity and duration of the gene silencing needs to be optimized. Optimization of the "gene silencing" effects has been extensively studied to find the optimal sequence of siRNA (Reynolds et al., 2004; Yoshinari et al., 2004), which determines the intensity of gene silencing by siRNA. When siRNA with an optimized sequence is introduced to cells via a suitable delivery agent, the expression of a specific protein is markedly reduced by degrading the targeted mRNA. However, the expression level of the target gene will return to a normal level, because siRNA is degraded and its effective concentration in the cells decreases with time. To use siRNA for silencing target gene expression, therefore, it is very important to understand how long the target mRNA or protein is suppressed by the siRNA introduced.

Maximal inhibitory efficiency of siRNA, a parameter that has frequently been used to express the potency of each siRNA, should be discussed with the duration or persistence of its effect. In the present study, therefore, we developed a simple kinetic analytical method based on moment analysis to quantitatively assess both the intensity and duration of gene silencing by siRNA. A murine melanoma cell line (B16-BL6) was stably transfected with firefly (target gene of RNAi) and sea pansy (internal standard gene) *luciferase* genes (B16-BL6/dual Luc). B16-BL6/dual Luc was used to monitor the gene silencing. In this cell line, gene expression was evaluated by the ratio of the firefly luciferase activity to that of sea pansy luciferase, because the luciferase activity is proportional to the amount of luciferase protein and the half-life of the firefly luciferase is short enough to reflect the time-course of the mRNA level. The time-course of the reduction in protein expression was characterized by the proposed kinetic analysis, which provides important parameters to evaluate the intensity and duration of gene silencing by siRNA.

Correspondence to: Y. Takakura

MATERIALS AND METHODS

Construction of Stably Expressing Cell Lines

B16-BL6/dual Luc, a cell line that expresses both firefly and sea pansy *luciferase*, was constructed from a murine melanoma cell line B16-BL6 (Poste et al., 1980) as reported previously (Takahashi et al., 2005). The cells were cultured in Dulbecco's modified Eagle's minimum essential medium (Nissui Pharmaceutical, Tokyo, Japan) supplemented with 10% fetal bovine serum (FBS) and penicillin/streptomycin/L-glutamine (PSG) at 37°C and 5% CO_2. B16-BL6/dual Luc continuously expressed the firefly and sea pansy luciferases activities at about 3 and 10 RLU/s/cell, respectively.

siRNA

Synthetic siRNA targeting the mRNA of firefly *luciferase*$^+$ (target sequence: GTG CGC TGC TGG TGC CAA CCC) was purchased from Takara Bio (Otsu, Japan).

Transfection

B16-BL6/dual Luc cells were plated on 24-well culture plates (at a density of 2×10^4 cells/well). After an overnight incubation, the transfection of siRNA was performed using Lipofectamine 2000 at a final concentration of 2 μg/mL according to the manufacturer's instructions. Plasmid DNA without specific expression was used to transfect an equal amount of nucleotides, since the amount of nucleotides contained in Lipofectamine 2000 complex affect cell activity. In brief, 1 μg of nucleotides was mixed with 3 μg Lipofectamine 2000, and the resulting complex was added to the cells. Cells were incubated with the complex for 4 h and then cells were cultured with culture medium as described above.

Luciferase Assay

To determine luciferase activity, B16-BL6/dual Luc cells were lysed using the cell lysis buffer of an assay kit (PiccageneDual, Toyo Ink, Tokyo, Japan). Then, samples were mixed with the kit luciferase assay buffer, and the chemiluminescence produced was measured in a luminometer (Lumat LB9507, EG and G Berthold, Bad Wildbad, Germany).

Following subtraction of the background activity using the lysates of B16-BL6 cells, the ratio of the activity of firefly luciferase to sea pansy luciferase was calculated to correct for differences in the number of cells in each sample. The ratios of luciferase activities were normalized with those of the cells transfected with only pDNA to give the parameter (R_{GE}: ratio of gene expression). R_{GE} was used as an indicator of the level of gene expression in B16-BL6/dual Luc cells.

Data Analysis

Gene silencing by siRNA was assumed to consist of two phases: the degradation phase of mRNA, in which siRNA degrades the target mRNA, and its recovery phase due to a reduction in the effective siRNA. When the ratio of gene expression is expressed as R_{GE}, the time-course of $(1-R_{GE})$ is predicted to construct a statistical distribution with respect to time. Thus, we define the area under the curve of the inhibitory effect (AUC_{IE}) as an index of the total intensity of RNAi and the mean response time of the inhibitory effect (MRT_{IE}) as an index of its duration by Equations (1) and (2), respectively.

$$AUC_{IE} = \int_0^\infty (1 - R_{GE})dt \tag{1}$$

$$MRT_{IE} = \frac{\int_0^\infty t \cdot (1 - R_{GE})dt}{\int_0^\infty (1 - R_{GE})dt} \tag{2}$$

The numerical calculation is the same as that used for the area under the plasma concentration-time curve (AUC) and the mean residence time (MRT) by trapezoidal integration (Yamaoka et al., 1978). Taking siRNA as a drug and AUC or MRT as the response to the drug, we assumed that AUC_{IE} and MRT_{IE} versus the initial concentration of siRNA (C_0) could be expressed by the following linearized equation, which is known to describe the dose–response curves of drugs. The parameters a and b were estimated by linearizing the plots.

$$\frac{C_0}{AUC_{IE}} \text{ or } \frac{C_0}{MRT_{IE}} = \frac{C_0}{a} + \frac{b}{a} \tag{3}$$

RESULTS AND DISCUSSION

Figure 1 shows the time-courses of the gene expression level of firefly luciferase in B16-BL6/dual Luc cells following transfection of siRNA at an initial concentration (C_0) of 1, 10, or 100 nM. When the C_0 was 1 or 10 nM, the expression ratio decreased with time, and reached a minimum at 2 days following transfection. On the other hand, at the highest concentration of 100 nM, R_{GE} had a flat trough from day 1 to 6, indicating saturation of the RNAi effect.

The suppression was significant until day 3 for 1 nM, day 5 for 10 nM, and day 8 for 100 nM of siRNA at a 5% level of significance (Student's *t*-test). Table I summarizes the AUC_{IE} and MRT_{IE} calculated by Equations (1) and (2); both the AUC_{IE} and MRT_{IE} increased as the C_0 increased. C_0/AUC_{IE} and C_0/MRT_{IE} versus C_0 are shown in Figures 2 and 3. The correlation coefficients (r) of both C_0/AUC_{IE} and C_0/MRT_{IE} versus C_0 were more than 0.999, and this equation can be converted to plots of the AUC_{IE} and MRT_{IE}, respectively, versus the $\log C_0$ where both the AUC_{IE} and MRT_{IE} have a sigmoidal shape when plotted against $\log C_0$.

Time-dependent changes in RNAi effect and kinetic analysis of the effect have been reported in the literature (Hahn et al., 2004; Haley and Zamore, 2004; Raab and Stephanopoulos, 2004). To determine the optimal time point for mRNA analysis by qRT-PCR, Hahn et al. (2004) studied the kinetics of mRNA degradation caused by siRNA. They

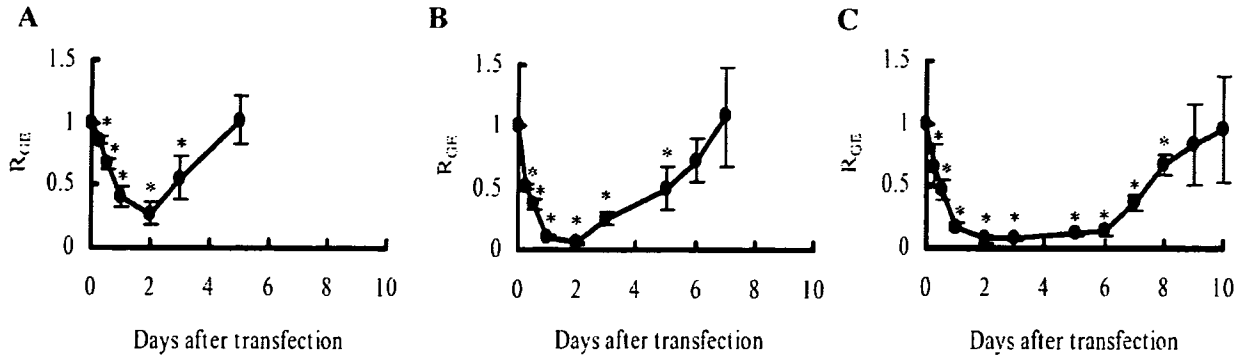

Figure 1. Time-courses of gene expression (R_{GE}) following transfection of siRNA. B16-BL6/dual Luc cells were transfected with siGL3 at concentrations of 1 (**A**), 10 (**B**), and 100 nM (**C**). Luciferase activities were determined at the indicated times after transfection. The results are expressed as mean ± SD ($n = 3$). *, $P < 0.05$ for Student's t-test versus control group.

focused only on the initiation of RNAi (mRNA degradation phase), and did not investigate the later phase. From a kinetic viewpoint, Haley et al. characterized the interaction between siRNA and the siRNA-directed ribonucleoprotein complex (RISC) that catalyzes a target RNA cleavage in the RNAi pathway (Haley and Zamore, 2004). They investigated mainly the time-course of the degradation of the RNA siRNA-RISC complex, and it was found that RISC is a classical Michaelis–Menten enzyme in the presence of ATP. They further suggested that different regions of siRNA play their own roles in the cycle of target recognition, cleavage, and target recognition. However, the goal of their study was to characterize the siRNA–RISC complex, which was different from our goal of quantitatively describing the intensity and duration of siRNA-based gene silencing. Therefore, their study was limited to using cell extracts as the RNAi machinery and they did not study the induction of RNAi in living cells. The kinetics of transgene expression was discussed after the cotransfection of pDNA encoding reporter gene and the corresponding specific siRNA (Raab and Stephanopoulos, 2004). They attempted to predict the time-course of the transgene expression resulting from the transfection of pDNA and siRNA-based transcript degradation. In order to achieve this, they assumed a model that describes the dynamics of mRNA transcript, protein, plasmid DNA, and transfected siRNA. It was demonstrated in their study that different profiles of exogenous gene expression can be obtained depending on the time when the siRNA is transfected after the transfection of the target plasmid, and the profiles can be predicted by the proposed mathematical model. However, their investigation was limited to a discussion of the effect of siRNA on the kinetics of exogenous gene expression.

Table I. AUC_{IE} (day) and MRT_{IE} (day) versus siRNA initial concentrations (C_0; nM).

C_0	AUC_{IE}	MRT_{IE}
1	2.00	1.98
10	4.00	2.72
100	6.59	4.21

Unlike these earlier studies, we investigated the time-course of the RNAi effect on endogenous gene expression from the beginning to the end of the effect. Moreover, our study provides a method to evaluate kinetically the intensity and duration of the RNAi effect based on moment analysis. In a recent paper, Kim et al. (2005) reported that synthetic RNA duplexes 25–30 nucleotides in length can be up to 100-fold more potent than corresponding conventional 21-mer siRNAs. The increase in the efficacy was estimated by the dose–response data on the level of protein expression of enhanced green fluorescent protein (EGFP) at a single (24 h) time point. However, the results shown in Figure 3 in the reference indicated that the difference in the RNAi effect between a 21-mer siRNA and a 27-mer double stranded RNA (dsRNA) was not so large as the value (100-fold) estimated from EGFP at 24 h. Assuming that the EGFP level returns to the initial level (100%) with the same slope as that observed between day 8 and 10, we calculated the AUC_{IE} using the method developed in the present study to be 3.11 and 10.8 for

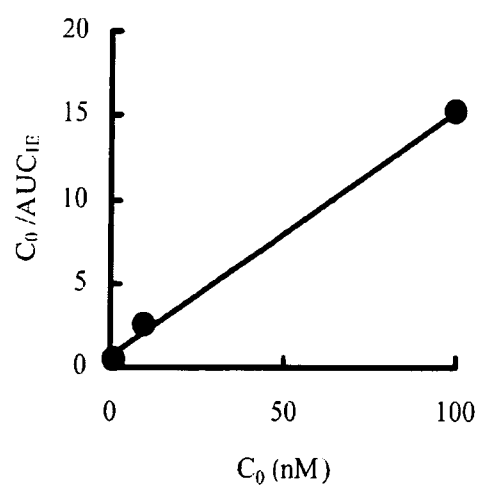

Figure 2. Linear plots of C_0/AUC_{IE} versus C_0. Symbols represent C_0/AUC_{IE} calculated by Equation (1), with lines fitted using Equation (3). a and b, are parameters described in Equation (3), and were calculated to be 6.90 and 4.72, respectively. r, is the correlation coefficient of the linear plots, and was calculated to be 0.999.

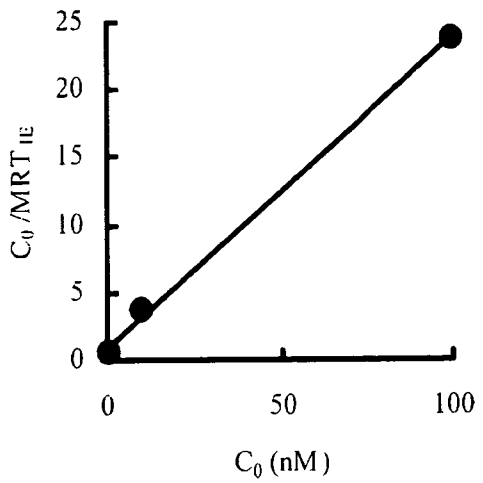

Figure 3. Linear plots of C_0/MRT_{IE} versus C_0. Symbols represent C_0/MRT_{IE} calculated by Equation (2), with lines fitted using Equation (3). *a* and *b*, are parameters described in Equation (3), and were calculated to be 4.35 and 3.47, respectively. r, is the correlation coefficient of linear plots, and was calculated to be 0.999.

the 21-mer siRNA and the 27-mer dsRNA, respectively, indicating that the 27-mer siRNA is only threefold more potent than the conventional one, as far as the total RNAi potency is evaluated by the AUC_{IE}. The MRT_{IE} calculated (3.82 for the 21-mer siRNA and 6.47 for the 27-mer dsRNA) also indicated a moderate increase. These findings strongly suggest that the AUC_{IE} and MRT_{IE} are useful parameters to quantitatively compare the potency of various types of RNAi effectors including ones that will be developed in future.

In conclusion, the AUC_{IE} and MRT_{IE} proposed in this study can be calculated by simple numerical integration. The AUC_{IE} can be used as an index of the intensity of gene silencing effect of siRNA delivered, whereas MRT_{IE} can be used for the duration of the RNAi effect. The time-course of the reduction in protein expression by siRNA was successfully evaluated by the proposed kinetic analysis, thereby providing important parameters to evaluate the extent and duration of gene silencing by siRNA and to quantitatively understand and efficiently control RNAi. Also, these parameters will be useful for predicting the duration of the gene silencing effect of siRNA before applying it as an experimental tool as well as a therapeutic treatment. Moreover, our proposed moment analysis is suitable for designing experimental or therapeutic protocols in which siRNA is administered repeatedly to obtain a sustained gene silencing effect as well as providing well-controlled experimental conditions or a good therapeutic effect.

References

Caplen NJ, Parrish S, Imani F, Fire A, Morgan RA. 2001. Specific inhibition of gene expression by small double-stranded RNAs in invertebrate and vertebrate systems. Proc Natl Acad Sci USA 98:9742–9747. Epub 2001 Jul 31.

Elbashir SM, Harborth J, Lendeckel W, Yalcin A, Weber K, Tuschl T. 2001. Duplexes of 21-nucleotide RNAs mediate RNA interference in cultured mammalian cells. Nature 411:494–498.

Hahn P, Schmidt C, Weber M, Kang J, Bielke W. 2004. RNA interference: PCR strategies for the quantification of stable degradation-fragments derived from siRNA-targeted mRNAs. Biomol Eng 21:113–117.

Haley B, Zamore PD. 2004. Kinetic analysis of the RNAi enzyme complex. Nat Struct Mol Biol 11:599–606. Epub 2004 May 30.

Kim DH, Behlke MA, Rose SD, Chang MS, Choi S, Rossi JJ. 2005. Synthetic dsRNA Dicer substrates enhance RNAi potency and efficacy. Nat Biotechnol 23:222–226. Epub 2004 Dec 26.

McManus MT, Sharp PA. 2002. Gene silencing in mammals by small interfering RNAs. Nat Rev Genet 3:737–747.

Milhavet O, Gary DS, Mattson MP. 2003. RNA interference in biology and medicine. Pharmacol Rev 55:629–648.

Miyagishi M, Hayashi M, Taira K. 2003. Comparison of the suppressive effects of antisense oligonucleotides and siRNAs directed against the same targets in mammalian cells. Antisense Nucleic Acid Drug Dev 13:1–7.

Poste G, Doll J, Hart IR, Fidler IJ. 1980. In vitro selection of murine B16 melanoma variants with enhanced tissue-invasive properties. Cancer Res 40:1636–1644.

Raab RM, Stephanopoulos G. 2004. Dynamics of gene silencing by RNA interference. Biotechnol Bioeng 88:121–132.

Reynolds A, Leake D, Boese Q, Scaringe S, Marshall WS, Khvorova A. 2004. Rational siRNA design for RNA interference. Nat Biotechnol 22:326–330. Epub 2004 Feb 1.

Takahashi Y, Nishikawa M, Kobayashi N, Takakura Y. 2005. Gene silencing in primary and metastatic tumors by small interfering RNA delivery in mice: Quantitative analysis using melanoma cells expressing firefly and sea pansy luciferases. J Control Release 105:332–343.

Tuschl T, Zamore PD, Lehmann R, Bartel DP, Sharp PA. 1999. Targeted mRNA degradation by double-stranded RNA in vitro. Genes Dev 13: 3191–3197.

Yamaoka K, Nakagawa T, Uno T. 1978. Statistical moments in pharmacokinetics. J Pharmacokinet Biopharm 6:547–558.

Yoshinari K, Miyagishi M, Taira K. 2004. Effects on RNAi of the tight structure, sequence and position of the targeted region. Nucleic Acids Res 32:691–699. Print 2004.

Zamore PD, Tuschl T, Sharp PA, Bartel DP. 2000. RNAi: Double-stranded RNA directs the ATP-dependent cleavage of mRNA at 21 to 23 nucleotide intervals. Cell 101:25–33.

THE JOURNAL OF GENE MEDICINE
J Gene Med 2006; 8: 53–62.
Published online 25 July 2005 in Wiley InterScience (www.interscience.wiley.com). DOI: 10.1002/jgm.812

RESEARCH ARTICLE

Use of lipoplex-induced nuclear factor-κB activation to enhance transgene expression by lipoplex in mouse lung

Takeshi Kuramoto[1]
Makiya Nishikawa[2]*
Oranuch Thanaketpaisarn[1]
Takayuki Okabe[1]
Fumiyoshi Yamashita[1]
Mitsuru Hashida[1]

[1]*Department of Drug Delivery Research, Graduate School of Pharmaceutical Sciences, Kyoto University, Sakyo-ku, Kyoto 606-8501, Japan*

[2]*Department of Biopharmaceutics and Drug Metabolism, Graduate School of Pharmaceutical Sciences, Kyoto University, Sakyo-ku, Kyoto 606-8501, Japan*

*Correspondence to:
Makiya Nishikawa, Department of Biopharmaceutics and Drug Metabolism, Graduate School of Pharmaceutical Sciences, Kyoto University, Sakyo-ku, Kyoto 606-8501, Japan. E-mail: makiya@pharm.kyoto-u.ac.jp

Received: 4 September 2004
Revised: 19 April 2005
Accepted: 23 May 2005

Abstract

Background Although lipofection-induced TNF-α can activate nuclear factor κB (NF-κB), which, in turn, increases the transgene expression from plasmid DNA in which any NF-κB responsive element is incorporated, no attempts have been made to use such biological responses as NF-κB activation against a vector to enhance vector-mediated gene transfer.

Methods A lipoplex composed of *N*-[1-(2,3-dioleyloxy)propyl]-*N*,*N*,*N*-trimethylammonium and cholesterol liposome and plasmid DNA encoding firefly luciferase under the control of the cytomegalovirus immediate early promoter (pCMV-Luc) was intravenously injected into mice. Luciferase activity as well as NF-κB activation in the lung were evaluated. Then, a novel plasmid DNA, pCMV-κB-Luc, was constructed by inserting 5 repeats of NF-κB-binding sequences into the pCMV-Luc.

Results NF-κB in the lung was activated by injection of the lipoplex and its nuclear localization was observed. An injection of lipopolysaccharide 30 min prior to the lipofection further activated NF-κB. At the same time, the treatment significantly increased the transgene expression by lipoplex, suggesting a positive correlation between expression and NF-κB activity. Based on these findings, we tried to enhance the lipoplex-based transgene expression by using NF-κB activation. The lipoplex consisting of pCMV-κB-Luc showed a 4.7-fold increase in transgene expression in the lung compared with that with pCMV-Luc.

Conclusions We demonstrated that NF-κB activation by lipoplex can be used to enhance lipoplex-mediated transgene expression by inserting NF-κB-binding sequences into plasmid DNA. These findings offer a novel method for designing a vector for gene transfer in conjunction with biological responses to it. Copyright © 2005 John Wiley & Sons, Ltd.

Keywords lipoplex; TNF-α; NF-κB; lung; plasmid DNA; CMV promoter

Introduction

The cationic liposome/plasmid DNA complex, or lipoplex, is a safe and convenient nonviral vector that has been intensively studied for *in vivo* gene transfer [1–3]. However, it has some drawbacks, such as a low level of transgene expression, which is mainly attributed to the biological barrier preventing exogenous plasmid DNA passing through biological membranes such as the plasma and endosomal membranes, and the nuclear envelope [4,5]. The use of dioleoyl phosphatidylethanolamine (DOPE) as a helper

lipid in cationic liposome formulations can improve the delivery of plasmid DNA into the cytoplasm through destabilization of the endosomal membrane, leading to increased transgene expression. Intratracheal or intratissue gene transfer using lipoplex formulated with DOPE-containing cationic liposomes has been shown to be very efficient. However, such lipoplexes induce fusion of erythrocytes and produce less transgene expression after systemic administration [6].

Another drawback is the nonspecific and systemic production of inflammatory cytokines such as tumor necrosis factor (TNF)-α, interferon (IFN)-γ and interleukin (IL)-12, mostly induced by the unmethylated CpG motif contained in plasmid DNA [7–9]. Kupffer cells in the liver are the major source of these cytokines after intravenous injection of lipoplex [10]. Excessive production of such cytokines can be regarded as a side effect of lipofection and should be reduced as much as possible. Various approaches have been designed to decrease cytokine production, including a reduction in the number of immunostimulatory CpG motifs [11], the use of PCR-amplified DNA fragments [12], and sequential injection of cationic liposomes and plasmid DNA [13].

On the other hand, biological responses such as cytokine production may be used to enhance the transgene expression by lipoplex. Of the cytokines induced by lipoplex, TNF-α is a well-known activator of the transcription factor nuclear factor κB (NF-κB) that is present in the cytoplasm of a variety of cells [14–16]. Upon activation NF-κB translocates and accumulates in the nucleus, binds to its recognition DNA element, and participates in the activation of transcription of various genes [17]. Genes activated by NF-κB include cell-surface molecules such as immunoglobulin κ light chain, class I and II major histocompatibility complex, and various cytokines. In addition, some viruses including cytomegalovirus (CMV) have also NF-κB-binding sites in their enhancers, and viral production is stimulated by agents that activate NF-κB [18].

These pieces of evidence have led us to form a hypothesis that lipofection-induced TNF-α activates NF-κB in target cells, which, in turn, increases the transgene expression from plasmid DNA in which any NF-κB-responsive element is incorporated. However, no attempts have been made to use such biological responses as NF-κB activation against a vector to enhance vector-mediated gene transfer. In the present study, therefore, we first investigated whether NF-κB in the lung was activated after intravenous injection of a lipoplex. Plasmid DNA encoding firefly luciferase under the control of CMV immediate early promoter (pCMV-Luc) was used as a model plasmid, and *N*-[1-(2,3-dioleyloxy)propyl]-*N*,*N*,*N*-trimethylammonium (DOTMA) and cholesterol (Chol) liposomes (DOTMA/Chol liposomes) were prepared as cationic liposomes. To examine the correlation between NF-κB activation and transgene expression, we examined the effect of lipopolysaccharide (LPS), a well-known activator of NF-κB, and found a positive correlation between the activation and transgene expression in the lung. Based on these findings, we constructed a novel plasmid DNA, pCMV-κB-Luc, by inserting 5 additional NF-κB-binding sequences into the pCMV-Luc, and achieved significantly enhanced transgene expression in the lung by intravenous injection of a lipoplex containing the novel plasmid DNA.

Materials and methods

Chemicals

DOTMA was purchased from Tokyo Kasei (Tokyo, Japan). Chol was purchased from Nacalai Tesque (Kyoto, Japan). LPS was purchased from Sigma (St. Louis, MO, USA). ^{111}Indium chloride was supplied by Nihon Medi-Physics Co. (Takarazuka, Japan). [γ-^{32}P]ATP was purchased from Amersham (Tokyo, Japan). PathDetect® NF-κB *cis*-reporting pNF-κB-Luc plasmid was purchased from Stratagene (La Jolla, CA, USA). Opti-MEM I was obtained from Gibco BRL (Grand Island, NY, USA). The nuclear extract kit was supplied from Active motif. Oligonucleotides were purchased from Sawady (Tokyo, Japan); one with a NF-κB-binding sequence (5′-TCAGAGGGGACTTTCCGAGAGG-3′, the underlined part represents the NF-κB-binding sequence) and one with a random sequence (5′-AGTGTCAGCACGTGGAGATGCG-3′) were used. All other chemicals were of the highest purity available.

Plasmid DNA

pCMV-Luc was constructed by inserting the *Hind*III/*Xba*I firefly luciferase cDNA fragment from pGL3-control vector (Promega, Madison, WI, USA) into the *Hind*III/*Xba*I site of pcDNA3 vector (Invitrogen, Carlsbad, CA, USA) as previously reported [6]. pCMV-κB-Luc was constructed by inserting the *Bgl*II/*Nru*I site of the 5 repeats of the NF-κB-binding sequence from pNF-κB-Luc into the *Bgl*II/*Nru*I site of pCMV-Luc. Each plasmid DNA was amplified in the *E. coli* strain DH5α and then isolated and purified using a Qiagen Endofree™ Plasmid Giga kit (Qiagen GmbH, Hilden, Germany). The LPS concentration in plasmid DNA was measured with a LAL assay kit (Limus F Single Test Wako; Wako Pure Chemical, Osaka, Japan) and found to be less than 22 pg/μg DNA. Then purified plasmid DNA was dissolved in sterilized endotoxin-free 5% dextrose and stored at −20 °C until required.

Preparation of cationic liposomes

A mixture of 15.2 mg DOTMA and 8.8 mg Chol in 12 ml chloroform was dried as a thin film, vacuum desiccated, and hydrated with vortexing in 3 ml sterilized 5% dextrose to give a final concentration of 3.5 mg DOTMA/ml in a 50-ml round-bottomed flask [10]. After hydration, the dispersion was sonicated for 3 min in a bath sonicator at

37 °C. The lipid solution was frozen in liquid nitrogen for 2 min and thawed in a water bath for 6 min at 37 °C. The dispersion was passed through a MILLEX®-GV 0.22 μm filter unit (Millipore, Bedford, MA, USA). The particle size of the cationic liposomes was found to be about 160 nm by dynamic light scattering spectrophotometry (LS-900, Otsuka Electronics, Osaka, Japan). The lipid concentration was determined by the Cholesterol C-II Test Wako (Wako Pure Chemical, Osaka, Japan).

Preparation of lipoplex

The liposome dispersion (4.5 mg/ml) was diluted to 1.25 mg/ml and 2 mg plasmid DNA/ml solution were diluted with 5% dextrose to 0.25 mg/ml. An equal volume of each diluted solution was mixed in a water bath at 37 °C and allowed to stand for 30 min. The particle size of the lipoplex was measured in 5% dextrose and found to be about 250 nm in diameter.

Animal experiments

Male ddY and male BALB/c mice were purchased from the Shizuoka Agricultural Co-operative Association for Laboratory Animals (Shizuoka, Japan) and maintained on a standard food and water diet under conventional housing conditions. All animal experiments were conducted in accordance with the principles and procedures outlined in the National Institutes of Health Guide for the Care and Use of Laboratory Animals. The protocols for animal experiments were approved by the Animal Experimentation Committee of the Graduate School of Pharmaceutical Sciences of Kyoto University.

Tissue distribution after intravenous injection of lipoplex

Plasmid DNA (pCMV-Luc) was radiolabeled with ^{111}In as reported elsewhere [19]. Then ^{111}In-plasmid DNA was diluted with nonradiolabeled plasmid DNA to give a dose of plasmid DNA of 25 μg/mouse. Male ddY mice (20–22 g) received the lipoplex containing ^{111}In-plasmid DNA in sterilized 5% dextrose by tail vein injection. Mice were killed at 1, 10, 60 and 120 min after injection and the liver, kidney, spleen, lung, and heart were harvested, rinsed with saline and weighed. Blood was withdrawn from the vena cava and urine was collected from the bladder. The ^{111}In-radioactivity of the samples was counted in a well-type scintillation counter (ARC-500, Aloka, Tokyo, Japan).

In vivo transfection and reporter gene assay

Male BALB/c mice (20 g) received lipoplex at a dose of 25 μg plasmid DNA/mouse in 200 μl 5% dextrose by tail vein injection. At indicated times after injection, the lung was harvested, washed with ice-cold saline, and homogenized with 4 ml/g tissue of lysis buffer (0.1 M Tris, 0.05% Triton X-100, 2 mM EDTA, pH 7.8), and subjected to three cycles of freezing in liquid nitrogen for 3 min and thawing in a water bath at 37 °C for 3 min. The homogenates were centrifuged at 10 000 *g* for 8 min at 4 °C. Then, 10 μl of the supernatant were mixed with 100 μl luciferase assay buffer (Pikkagene, Toyo Ink, Tokyo, Japan) and the chemiluminescence was measured with a luminometer (Lumat LB 9507, EG&G Bethhold, Bad Wildbad, Germany).

Separately, naked plasmid DNA dissolved in a 1.6 ml saline was injected into the tail vein of mice within 5 s at a dose of 1 μg plasmid DNA/mouse [20]. At 6 h after injection, the lung and liver were excised and the luciferase activity was assayed as above.

Cytokine assay

The levels of TNF-α in serum after intravenous injection of the lipoplex were measured using an ELISA kit (AN'ALYZA™, Genzyme, Cambridge, MA, USA) as described previously [21]. Blood was collected into plastic tubes from the vena cava of mice under anesthesia, and allowed to stand for 3 h at 4 °C. Then the samples were centrifuged at 3000 *g* for 30 min at 4 °C and the serum obtained was used for the assay.

Preparation of nuclear protein extracts

Mice were killed at the indicated times after injection of the lipoplex and the lungs were immediately harvested and frozen in liquid nitrogen. Nuclear protein extracts were prepared as described previously [22]. In brief, each lung was immersed in 1 ml of ice-cold lysis buffer (10 mM Hepes, pH 7.9, 10 mM KCl, 1.5 mM $MgCl_2$, 0.5 mM DTT, 0.5 mM PMSF, 2 μg/ml pepstatin A, 2 μg/ml leupeptin, 2 μg/ml L-leucinethiol) and homogenized on ice with a Potter homogenizer. It was then incubated on ice for 15 min and 25 μl of 10% Nonidet P-40 (Sigma Aldrich Japan, Tokyo, Japan) were added. After vortexing for 15 s, the samples were incubated on ice for 20 min and centrifuged at 10 000 *g* for 15 min at 4 °C. The pelleted nuclei were resuspended in 100 μl of extraction buffer (20 mM Hepes, pH 7.9, 420 mM NaCl, 1.5 mM $MgCl_2$, 0.2 mM EDTA, 0.5 mM DTT, 0.5 mM PMSF, 2 μg/ml pepstatin A, 2 μg/ml leupeptin, 2 μg/ml L-leucinethiol) and incubated on ice for 30 min. The nuclear suspension was centrifuged at 10 000 *g* for 15 min at 4 °C to collect the supernatant containing nuclear protein extracts. The concentration of nuclear protein in the resulted supernatant from each lung extract was determined with the Protein Quantification Kit-Wide range (Dojindo Molecular Technologies, Inc., Kumamoto, Japan). Separately, colon26 cells were treated with 4 μM phenazine methosulfate to activate NF-κB, and nuclear

protein extracts from the cells were collected using a nuclear extract kit (Active motif, CA, USA), which were used for the comparison of plasmid DNA in the binding strength to activated NF-κB.

Electrophoretic mobility shift assay (EMSA)

EMSA was performed as described previously [23]. A single-stranded oligonucleotide containing an NF-κB-binding sequence (5′-TCAGAGGGGACTTTCCGAGAGG-3′) was end-labeled with [γ-^{32}P]ATP using polynucleotide kinase T4 (MEGALABEL™, Takara Bio Inc., Otsu, Japan). The end-labeled probe was purified from unincorporated [γ-^{32}P]ATP using Sephadex G-50 (Pharmacia, Uppsala, Sweden) and recovered in TNE buffer (10 mM Tris HCl, 0.1 M NaCl, 1 mM EDTA, pH 7.5). An aliquot of 50 μg extracted nuclear protein was incubated with 15 μl binding buffer (20 mM Hepes, pH 7.9, 0.5 mM EDTA, pH 8.0, 50 mM KCl, 10% glycerol, 0.5 mM DTT, 0.5 mM PMSF) and 2 μg salmon sperm DNA for 15 min on ice. Then 1×10^5 cpm of the radiolabeled oligonucleotide was added to the sample followed by an additional 30 min incubation at room temperature and 2 μl 0.1% bromphenol blue dye were added to each sample. An aliquot of 25 μl of the resulting solution was electrophoresed on a 4% nondenaturing polyacrylamide gel for 75 min at 150 V in TGE buffer. After completion of the electrophoresis, the gel was transferred to a piece of blotting paper and dried under vacuum. The dried gel was exposed to an Imaging Plate (Fuji Photo Film, Kanagawa, Japan) and analyzed by a Bio-Image analyzer system (BAS-2500, Fuji Photo Film).

Competitive EMSA

To compare the binding strength of plasmids with NF-κB, a competitive EMSA was carried out. An aliquot of 60 μg extracted nuclear protein from phenazine methosulfate treated colon26 cells was incubated with the 1.5×10^6 cpm of radiolabeled oligonucleotide on ice for 30 min with varying amounts of pCMV-Luc or pCMV-κB-Luc (0–0.3 μg/sample) in binding buffer as above. Then the samples (20 μl) were electrophoresed on a 4% nondenaturing polyacrylamide gel for 90 min at 150 V in a cold room. After completion of the electrophoresis, the gel was exposed as above and analyzed by a Bio-Image analyzer system (BAS-3000, Fuji Photo Film).

In vitro transfection and reporter gene assay

Cultured ECV304 cells were seeded at 2×10^5 cells per well onto 12-well plates 24 h before transfection. The cells were about 80% confluent at the time of transfection. Then, the cells were incubated with 1 ml Opti-MEM I containing 0.5 μg plasmid DNA complexed with DOTMA/Chol liposome for 4 h. Then the cells were incubated with or without TNF-α (25 ng/ml) for 3 h. After an additional 8 h incubation, the cells were scraped off the plates and centrifuged at 3000 *g* for 3 min at 4 °C. The pellets were resuspended in 1 ml phosphate-buffered slaine (PBS(-)) and subjected to three cycles of freezing and thawing. Aliquots of the supernatant were used to determine the luciferase activity with a luminometer as described above.

Separately, the cells were treated with the lipoplex for 2 h as described above. Then the cells were mixed with 2′,7′-dichlorodihydrofluorescein diacetate (Molecular Probes, Eugene, OR, USA), incubated for 30 min in 5% CO_2, humidified air at 37 °C, and examined under confocal microscopy. Once reactive oxygen species (ROS) were produced, a fluorescent product was generated.

Statistical analysis

The results are given as mean ± standard deviation (SD). Statistical analysis was performed using an unpaired *t*-test. For multiple comparison (Figure 3B), analysis of variance with subsequent Dunnett test was employed to determine the significance of differences. Values of $P < 0.05$ were considered statistically significant.

Results

Tissue distribution of lipoplex and serum TNF-α concentration

Luciferase activity in the lung peaked at 6–12 h after injection, then gradually decreased, showing a transient profile of transgene expression as reported previously (data not shown) [10,24]. Figure 1A shows the time-course of ^{111}In-radioactivity in the blood, liver, and lung after intravenous injection of a lipoplex prepared with DOTMA/Chol liposomes and ^{111}In-labeled plasmid DNA. As described previously [25], the lipoplex rapidly accumulated in the lung and then disappeared from the lung and was mainly delivered to the liver. Using the ^{111}In-labeling technique, the tissue distribution of the lipoplex can be traced longer than before, and it was shown that about 8% of the injected radioactivity remained in the lung at 6 h post-injection. About 50% of the injected radioactivity accumulated in the liver as early as 1 h after injection of the lipoplex. Previous studies in our laboratory showed that liver nonparenchymal cells are mainly involved in this uptake of lipoplex [26] and Kupffer cells in the liver are responsible for the production of TNF-α [10].

Figure 1B shows the time-course of the serum concentration of TNF-α after injection of the lipoplex. TNF-α could be detected as early as 1 h after injection, reaching a peak at 2 h with a value of more than 500 pg/ml, and

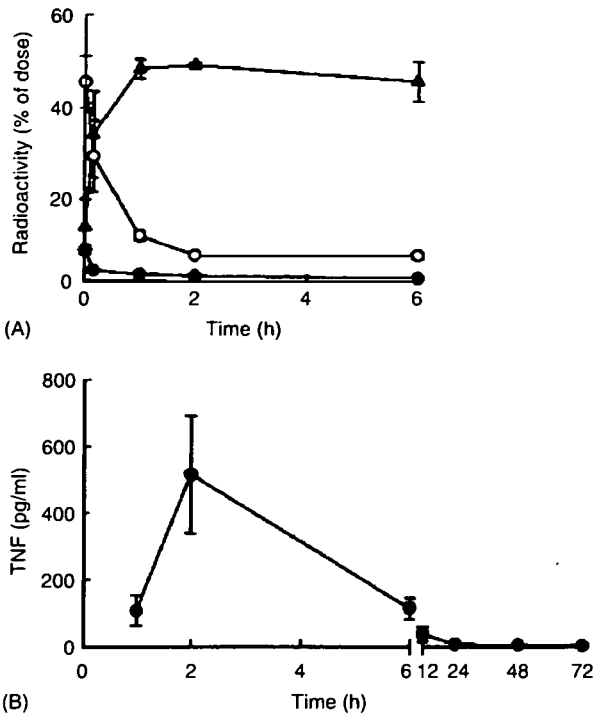

Figure 1. Tissue distribution of radioactivity after intravenous injection of ^{111}In-labeled lipoplex and serum concentration of TNF-α after intravenous injection of lipoplex in mice. (A) Mice received a DOTMA/Chol liposome-^{111}In-plasmid DNA complex at a dose of 25 μg plasmid DNA/mouse. Then blood concentration (●) and tissue accumulation in liver (▲) and lung (○) of radioactivity were determined at the indicated times. The results are expressed as the mean ± SD of three mice. (B) Time course of the serum concentrations of TNF-α after intravenous injection of the lipoplex at a dose of 25 μg plasmid DNA/mouse. At the indicated times post-injection, mice were killed and blood was collected. Serum concentrations of TNF-α were determined by ELISA. The results are expressed as the mean ± SD of three mice

then declining thereafter. At 24 h post-injection, TNF-α was barely detectable in serum.

NF-κB activation in mouse lung after intravenous injection of lipoplex

Activation of NF-κB was detected by an electrophoretic mobility shift assay (EMSA). Mouse lung was collected and homogenized, and the nuclear fractions were subjected to electrophoresis using ^{32}P-labeled oligonucleotide having an NF-κB-binding sequence. No NF-κB was found in the nuclear fraction of the lung from a control mouse (Figure 2, lane 1). On the other hand, NF-κB could be detected in the nuclear fraction of the lung 1 h after intravenous injection of the lipoplex into mice (Figure 2, lanes 2, 3), indicating that the lipoplex activates NF-κB in the lung. The amount of NF-κB detected was greater in mice receiving intravenous LPS 30 min prior to lipofection (Figure 2, lane 4).

The band was reduced by the addition of a 100-fold excess of oligonucleotide having an NF-κB-binding

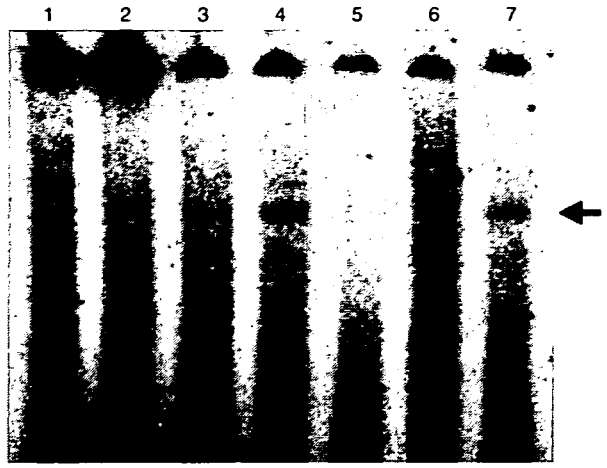

Figure 2. EMSA analysis of NF-κB in mouse lung after intravenous injection of lipoplex. Lane 1: Lung was harvested from untreated mice and nuclear protein extracts were analyzed by EMSA as a negative control. Lanes 2, 3: A pair of mice each received the lipoplex intravenously. One hour after injection, lungs were harvested and nuclear protein extracts were analyzed. Lane 4: Mice received 200 μg LPS 30 min before injection of the lipoplex. One hour after injection, lungs were harvested and nuclear protein extracts were analyzed. Lane 5: The sample from lane 4 was electrophoresed with a 100-fold excess of unlabeled oligonucleotide with an NF-κB-binding sequence. Lane 6: The sample from lane 4 was electrophoresed with a 100-fold excess of pCMV-Luc. Lane 7: The sample from lane 4 was electrophoresed with a 100-fold excess of unlabeled oligonucleotide with a random sequence

sequence to the nuclear extracts from the lipoplex-treated mice (Figure 2, lane 5), not by the addition of a random oligonucleotide (Figure 2, lane 7). These findings support the hypothesis that the band observed is specific to NF-κB. The addition of pCMV-Luc also resulted in disappearance of the band (Figure 2, lane 6). Therefore, this clearly shows that NF-κB binds to pCMV-Luc, probably through the NF-κB-binding sequences existing in the plasmid DNA. So far, it has been observed that NF-κB is activated in the lung by an intravenous injection of the lipoplex, and the activated NF-κB in the lung could affect the transgene expression in the organ.

Enhanced transgene expression through further activation of NF-κB by LPS

To investigate the relationship between the transfection efficiency and NF-κB activation in the lung, we examined the effect of the administration of LPS on transgene expression by the lipoplex. LPS was injected to exaggerate use for NF-κB activation in the lung. Mice receiving 200 μg LPS 30 min prior to the injection of the lipoplex showed a significantly greater transgene expression in the lung than those pre-injected with saline (Figure 3A). Next, LPS was injected after the injection of the lipoplex with different intervals between the injections. The injection of LPS after the lipoplex was also as effective as the

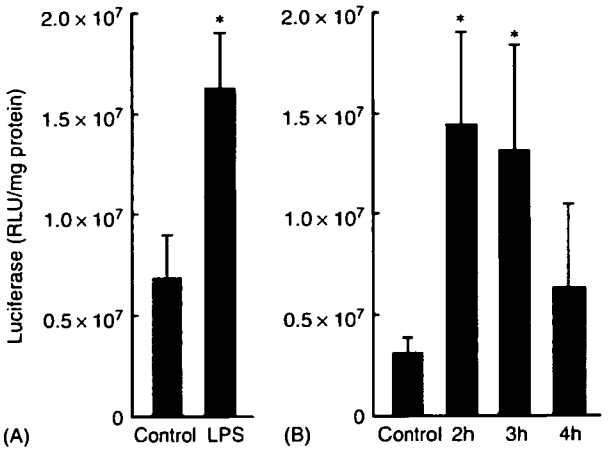

Figure 3. Luciferase activity in lung after intravenous injection of the lipoplex into mice receiving LPS pre- or post-injection. (A) At 30 min before injection of the lipoplex, mice received saline (control) or 200 μg LPS. At 6 h post-injection, mice were killed and the lungs were harvested for luciferase assay. (B) Mice received 200 μg LPS at the indicated times post-intravenous injection of the lipoplex. At 6 h post-injection, mice were killed and the lungs were harvested for luciferase assay. The results are expressed as the mean ± SD of four mice. *$P < 0.05$ vs. the control group

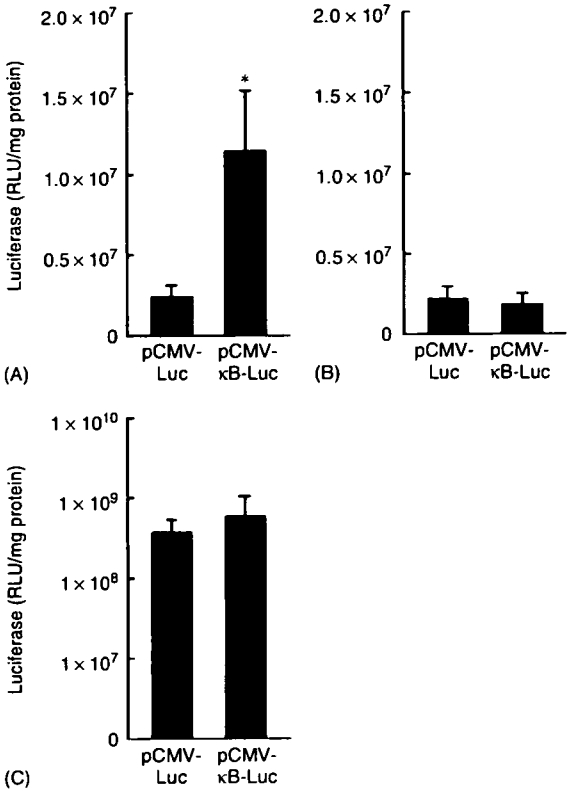

Figure 4. Luciferase activity in mouse lung by pCMV-Luc or pCMV-κB-Luc. (A) Each group of mice received a lipoplex composed of the indicated plasmid DNA at a dose of 25 μg DNA/mouse. At 6 h post-injection, mice were killed and the lungs were harvested for luciferase assay. The results are expressed as the mean ± SD of five mice. (B, C) Each group of mice received a large volume of saline containing the indicated plasmid DNA at a high velocity at a dose of 1 μg DNA/mouse. At 6 h post-injection, mice were killed and the lungs (B) and liver (C) were harvested for luciferase assay. The results are expressed as the mean ± SD of three mice

pre-injection method when the interval was 2 or 3 h (Figure 3B). However, injections at a 4 h interval did not significantly increase the expression. Together with the results of NF-κB activation by LPS (Figure 2, lane 4), these findings suggest that there should be a positive correlation between transgene expression and activation of NF-κB in the lung.

Enhanced transgene expression by lipoplex containing pCMV-κB-Luc

Taking the results of Figures 2 and 3 into consideration, we hypothesized that transgene expression by lipoplex is enhanced by use of activated NF-κB in the lung. Based on this, a novel plasmid vector, pCMV-κB-Luc, was constructed by inserting 5 repeats of an NF-κB-binding sequence upstream of the CMV promoter in pCMV-Luc, on the assumption that the inserted NF-κB-binding sequences would increase the opportunity of plasmid DNA interacting with the transcription factor. A lipoplex prepared with pCMV-κB-Luc showed a significantly greater (4.7-fold, $P < 0.05$) transgene expression in the lung after intravenous injection than that with pCMV-Luc (Figure 4A). Separately, naked plasmid DNA was injected into mice in a large volume of saline at a high velocity, a method which has proved a very powerful method for *in vivo* gene transfer to internal organs [20]. This procedure of gene transfer did not activate NF-κB in the lung (data not shown). Transgene expression by naked pCMV-κB-Luc was as great as that by naked pCMV-Luc in lung and liver (Figures 4B and 4C).

Transgene expression into cultured cells was also examined using ECV304 cells (Figure 5). Cells transfected with pCMV-κB-Luc showed a significantly greater transgene expression (2.14-fold, $P < 0.05$) than ones with pCMV-Luc. In addition, transgene expression by lipoplex containing pCMV-κB-Luc was further increased by the addition of TNF-α (Figure 5). Then, we measured the production of reactive oxygen species (ROS) in the cells. ECV304 cells were treated with the lipoplex for 2 h, then mixed with 2′,7′-dichlorodihydrofluorescein diacetate. We found that the addition of the lipoplex to the cells increased the fluorescent intensity in the cells, the indicator of intracellular ROS, another activator of NF-κB (Figure 6). The addition of the lipoplex induced intracellular ROS in other types of cells including a mouse macrophage cell line, RAW264.7 cells (data not shown).

Binding of NF-κB to pCMV-Luc and pCMV-κB-Luc

To confirm the stronger binding of pCMV-κB-Luc to NF-κB, a competitive EMSA was carried out (Figure 7).

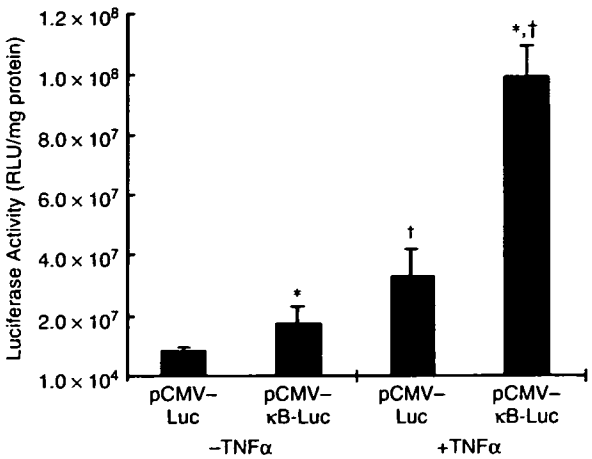

Figure 5. Luciferase activity in ECV304 cells by pCMV-Luc or pCMV-κB-Luc. ECV304 cells were transfected with a lipoplex consisting of the indicated plasmid DNA at a dose of 0.5 μg DNA/well for 4 h. TNF-α was added at a final concentration of 25 ng/ml and incubated for 3 h. After an additional 8 h of incubation, the luciferase activity was measured. The results are expressed as the mean ± SD of three wells. *$P < 0.05$ vs. pCMV-Luc group and †$P < 0.05$ vs. each control (without TNF-α treatment) group

Both pCMV-Luc and pCMV-κB-Luc reduced the specific binding of the radiolabeled probe to the nuclear extracts in a concentration (amount)-dependent manner. However, the reduction was more intense when pCMV-κB-Luc was added to the sample mixture. These results clearly demonstrate that pCMV-κB-Luc has greater binding ability with NF-κB than pCMV-Luc.

Discussion

Lipoplex-based transgene expression is considerably lower than that obtained with viral vectors. This can be explained by the fact that there are many biological barriers obstructing the access of plasmid DNA to the nucleus *in vivo* [27]; nucleases in the systemic circulation, the tangled structure of the extracellular matrix, degradation in the endosomes/lysosomes, and passage through the endosomal membrane and nuclear envelope. Some studies have investigated the physicochemical properties of lipoplex, and lipid composition of cationic liposomes has been optimized to overcome such barriers [28,29]. On the other hand, Zabner *et al.* [5] reported that the nuclear envelope is the main obstacle to lipofection. However, the details of the nuclear translocation of plasmid DNA are still unclear. Plasmid DNA is unlikely to passively diffuse into the nucleus, because its molecular size (usually <2000 kDa) is much greater than the passive diffusion limit (40–60 kDa) [30]. Some researchers reported that plasmid DNA is translocated into the nucleus through the nuclear pore complex (NPC) [31]. Macromolecules that use the NPC pathway have to be provided with a nuclear localization signal (NLS). However, plasmid DNA does not have any such signals, so this suggests that there may be a certain substance that provides plasmid DNA with a NLS. Dean *et al.* [31,32] reported that cytoplasmically microinjected plasmid DNA is translocated into the nucleus in association with several types of transcription factors (SP1, AP1, AP2, Oct-1, etc.). Such transcription factors bind to their corresponding sequences in plasmid DNA, and the transcription factor-associated plasmid DNA is translocated into the nucleus through the NPC. In the present study, we used a plasmid DNA, pCMV-Luc, that contains the CMV promoter, which has been reported to have 4 repeats of the NF-κB-binding sequences [33]. Therefore, it is possible that pCMV-Luc can be translocated into the nucleus through the activation of NF-κB. Mesika *et al.* [34] reported the NF-κB-assisted import of plasmid DNA into the nuclei of mammalian cells *in vitro*.

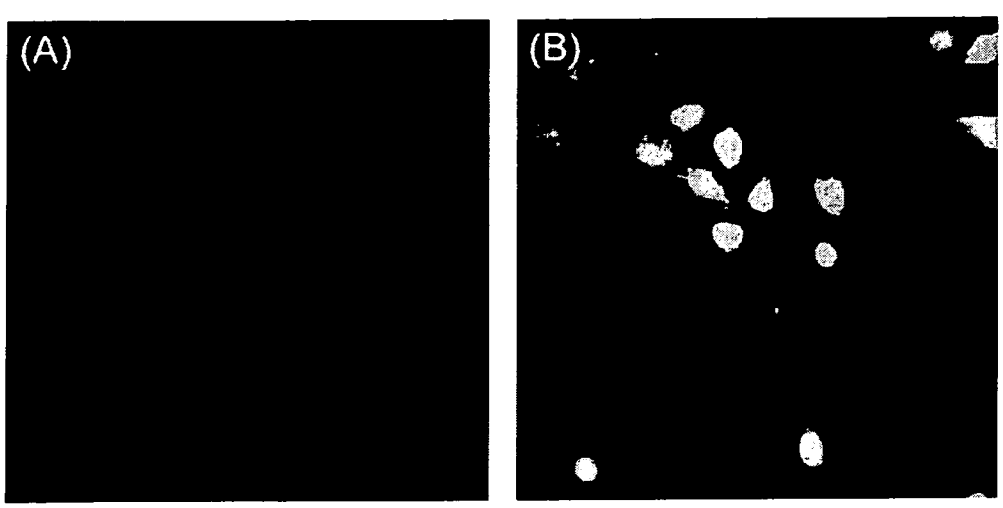

Figure 6. Confocal microscopic images of ECV304 cells treated with lipoplex. The cells were incubated with (B) or without the lipoplex (A, control) for 2 h and mixed with 2′,7′-dichlorodihydrofluorescein diacetate. Then, the cells were incubated for 30 min at 37 °C, and observed by confocal microscopy

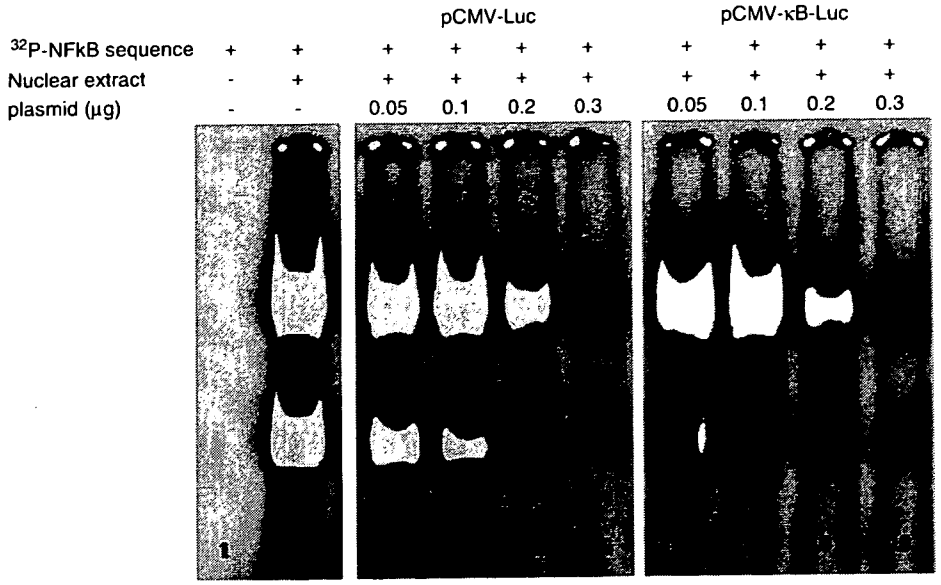

Figure 7. Inhibition of the binding of radiolabeled NF-κB concensus oligonucleotide with nuclear extracts by pCMV-Luc and pCMV-κB-Luc. Extracted nuclear protein from colon26 cells treated with phenazine methosulfate was incubated with the radiolabeled oligonucleotide with varying amounts of pCMV-Luc or pCMV-κB-Luc. Then the samples were electrophoresed on a 4% nondenaturing polyacrylamide gel for 90 min at 150 V in a cold room. After completion of the electrophoresis, the gel was exposed as above and analyzed by a Bio-Image analyzer system (BAS-3000, Fuji Photo Film)

In agreement with previous reports, our investigations showed that transgene expression was transient and greatest in the lung after intravenous injection of the lipoplex (data not shown). Intravenously injected lipoplexes became aggregated with erythrocytes or serum protein and entrapped in the capillaries of the lung, the first-pass organ after intravenous injection [25,35]. Most transgene expression occurred in the endothelial cells in this organ. In this study, we clearly demonstrated that only 8% of the injected lipoplex remained in the lung after intravenous injection and about 50% was delivered to the liver. The newly developed residualizing radiolabel [19] enabled us to trace the tissue distribution of the lipoplex for a much longer period after injection.

The fraction delivered to the liver was reported to be responsible for the production of inflammatory cytokines [10]. A significant level of TNF-α was observed in the serum after intravenous injection of the lipoplex. Serum TNF-α could be detected as early as 1 h after injection and peaked at 2 h then gradually diminished. Several reports claim that the production of TNF-α is mainly attributed to the unmethylated CpG motif contained in plasmid DNA [7–9]. Although several cytokines are produced by lipofection, we focused on TNF-α for the following reasons: (1) TNF-α is secreted primarily by macrophages recognizing a foreign substrate such as CpG motifs in plasmid DNA and IFN-γ or IL-12 are secreted thereafter [24]; (2) TNF-α plays a major role in cytokine-mediated cytotoxicity; and (3) TNF-α is one of the most potent stimulators of NF-κB [14–16]. In this study, we demonstrated that an injection of lipoplex activates NF-κB in the lung, the target organ for gene transfer (Figure 2, lanes 2, 3). To our knowledge, this is the first report showing that lipoplex activates NF-κB in the lung following administration. TNF-α secreted in the circulation should be involved in this activation. In addition to this pathway, the lipoplex might activate NF-κB by a direct pathway via an electrostatic interaction with the cell membrane, probably through the generation of ROS [36]. To examine this possibility, we added the lipoplex to ECV304 cells, a cell line possessing endothelial cell-like characteristics. We found that the lipoplex induced the production of a significant amount of intracellular ROS. These results suggest two possible pathways of NF-κB activation in the lung after *in vivo* lipofection: (1) NF-κB is directly activated by the lipoplex accumulated in the lung through ROS production and (2) NF-κB undergoes secondary activation by TNF-α in the circulation induced by lipofection. The previous study reported that pulmonary capillary endothelial cells appear to be more efficient at the nuclear transfer or gene expression process than the pulmonary epithelial cells after intravenous injection of a lipoplex [37]. In addition, activation of NF-κB by LPS or other stimuli has been demonstrated in cultured endothelial cells using EMSA [38]. Therefore, it is reasonable to speculate that the endothelial cells in the lung are the cells in which transgene expression as well as NF-κB activation take place after administration of lipoplex.

Tan *et al.* [21] previously reported that systemically produced TNF-α reduces transfection efficiency in the lung after *in vivo* lipofection. However, here we have shown that increased transgene expression was obtained after intravenous administration of LPS (Figure 3), during which a significant amount of TNF-α was secreted (data not shown). A possible explanation for this phenomenon

is that the CMV promoter is activated by NF-κB that has been activated by LPS-induced TNF-α [15,16]. The CMV promoter contains 4 repeats of NF-κB-binding sequences, which enable these two to interact with each other [33]. In Figure 2, significant activation of NF-κB was observed after intravenous administration of LPS (lane 4). In addition, the binding of NF-κB to pCMV-Luc was clearly demonstrated (Figure 2, lane 6). These findings support the experimental results showing that transgene expression by pCMV-Luc is positively correlated with the level of NF-κB activation in the lung. Observations from other studies also support these findings: CMV promoter activity was induced by inflammation in the rat arthritis model, where a positive correlation between transgene expression and the dose of LPS was obtained [39]. Reactivation of the previously silenced CMV promoter was observed after administration of LPS in mouse liver [40]. Finally, γ-irradiation enhanced transgene expression in leukemic cells only when a gene of interest was under the control of a CMV promoter [41]. Considering these previous observations and the current experimental finding that transgene expression and NF-κB activation in the lung are positively correlated (Figures 2 and 3), it is suggested that NF-κB activation plays an important role in transgene expression produced by lipofection.

Based on these findings, we hypothesized that transgene expression by lipofection can be enhanced by utilization of activated NF-κB. LPS cannot be used to activate NF-κB for practical situations because of its pyrogenic property. Instead, we constructed a novel plasmid DNA, pCMV-κB-Luc, by inserting 5 serial repeats of NF-κB-binding sequences upstream of the CMV promoter in pCMV-Luc. The competitive EMSA clearly demonstrated that insertion of the NF-κB-binding sequences can enhance the probability of interaction between NF-κB and plasmid DNA. As a result, the pCMV-κB-Luc-containing lipoplex showed a significantly greater transgene expression than that with pCMV-Luc in the lung (Figure 4A), as well as in cultured cells (Figure 5). Plasmid DNA should dissociate from the lipoplex to interact with activated NF-κB through its NF-κB-binding sequence. As shown in previous studies [42–44], plasmid DNA can be released from the lipoplex and the DNA released is transported into the nucleus. Therefore, any approach to facilitate the dissociation, such as the addition of polyethylene-glycol-modified ceramides into liposomes [45], may further improve the NF-κB-dependent increase in transgene expression by pCMV-κB-Luc. This enhanced transgene expression was probably achieved through an increased translocation of plasmid DNA into the nucleus by using the NLS of NF-κB, as suggested in a previous report [34]. The competitive EMSA would support this hypothesis (Figure 7).

Another explanation for the enhanced transgene expression is that the inserted NF-κB-binding sequences act as enhancers and directly upregulate the transcription of luciferase. However, this possibility is unlikely because of our data showing that gene transfer to the lung and liver following a naked pCMV-κB-Luc injection, where NF-κB was hardly activated, gave identical transgene expression to that obtained by a naked pCMV-Luc (Figures 4B and 4C). Tan *et al.* reported that co-injection of phosphorothioate oligonucleotides containing an NF-κB-binding sequence (NF-κB decoy) with lipoplex increased transgene expression in the lung [46]. Therefore, the inserted NF-κB-binding sequence may function as a molecular decoy for NF-κB, which could reduce NF-κB activation in the lung. However, stable oligonucleotides at high doses were required to reduce NF-κB activation [46], suggesting that the short NF-κB-binding sequence in the pCMV-κB-Luc will not act as a NF-κB decoy.

In conclusion, we clearly demonstrated that NF-κB in the lung is activated by an intravenous injection of the lipoplex. There was a positive correlation between transgene expression and NF-κB activation. Finally, we succeeded in constructing a novel and potent plasmid DNA with additional NF-κB-binding sequences that efficiently uses the NF-κB activated by the lipoplex to enhance transgene expression. These findings offer a novel strategy whereby a vector is designed to use the biological response against the vector itself. A better understanding of biological responses against various gene transfer approaches will provide us with useful information for designing a novel and potent approach to effective *in vivo* gene transfer.

Acknowledgements

This work was supported in part by Grants-In-Aid for Scientific Research from the Ministry of Education, Culture, Sports, Science and Technology, Japan, and by grants from the Ministry of Health, Labour and Welfare, Japan.

References

1. Luo D, Saltzman WM. Synthetic DNA delivery system. *Nat Biotechnol* 2000; **18**: 33–37.
2. Felgner PL. Nonviral strategies for gene therapy. *Sci Am* 1997; **276**: 102–106.
3. Felgner PL, Gadek TR, Holm M, *et al.* Lipofection: a highly efficient, lipid-mediated DNA-transfection procedure. *Proc Natl Acad Sci U S A* 1987; **84**: 7413–7417.
4. Subramanian A, Ranganathan P, Diamond SL. Nuclear targeting peptides for lipofection of nondividing mammalian cells. *Nat Biotechnol* 1999; **17**: 873–877.
5. Zabner J, Fasbender AJ, Moninger T, *et al.* Cellular and molecular barriers to gene transfer by a cationic lipid. *J Biol Chem* 1995; **270**: 18 997–19 007.
6. Sakurai F, Nishioka T, Saito H, *et al.* Interaction between DNA-cationic liposome complexes and erythrocytes is an important factor in systemic gene transfer via the intravenous route in mice: the role of the neutral helper lipid. *Gene Ther* 2001; **8**: 677–686.
7. Whitmore M, Li S, Huang L. LPD lipopolyplex initiates a potent cytokine response and inhibit tumor growth. *Gene Ther* 1999; **6**: 1867–1875.
8. Klinman DM, Yi AK, Beaucage SL, *et al.* CpG motifs present in bacterial DNA rapidly induce lymphocytes to secrete interleukin 6, interleukin 12 and interferon γ. *Proc Natl Acad Sci U S A* 1996; **93**: 2879–2883.
9. Krieg AM, Yi AK, Matson S, *et al.* CpG motifs in bacterial DNA trigger direct B cell activation. *Nature* 1995; **374**: 546–549.

10. Sakurai F, Terada T, Yasuda K, *et al.* The role of tissue macrophages in the induction of proinflammatory cytokine production following intravenous injection of lipoplexes. *Gene Ther* 2002; **9**: 1120–1126.
11. Yew NS, Zhao H, Wu IH, *et al.* Reduced inflammatory response to plasmid DNA vectors by elimination and inhibition of immunostimulatory CpG motifs. *Mol Ther* 2000; **1**: 255–262.
12. Hofman CR, Dileo JP, Li Z, *et al.* Efficient in vivo gene transfer by PCR amplified fragment with reduced inflammatory activity. *Gene Ther* 2001; **8**: 71–74.
13. Tan Y, Liu F, Li Z, *et al.* Sequential injection of cationic liposome and plasmid DNA effectively transfects the lung with minimal inflammatory toxicity. *Mol Ther* 2001; **3**: 673–682.
14. Lowenthal JW, Ballard DW, Bohnlein E, *et al.* Tumor necrosis factor alpha induces proteins that bind specifically to κB-like enhancer elements and regulate interleukin 2 receptor α-chain gene expression in primary human T lymphocytes. *Proc Natl Acad Sci U S A* 1989; **86**: 2331–2335.
15. Pahl HL. Activators and target genes of Rel/NF-κB transcription factors. *Oncogene* 1999; **18**: 6853–6866.
16. Karin M, Neriah YB. Phosphorylation meets ubiquitination: the control of NF-κB activity. *Ann Rev Immunol* 2000; **18**: 621–663.
17. Sha WC, Liou HC, Tuomanen EI, *et al.* Targeted disruption of the p50 subunit of NF-κB leads to multifocal defects in immune responses. *Cell* 1995; **80**: 321–330.
18. Griffin GE, Leung K, Folks TM, *et al.* Activation of HIV gene expression during monocyte differentiation by induction of NF-κB. *Nature* 1989; **339**: 70–73.
19. Nishikawa M, Nakano T, Okabe T, *et al.* Residualizing indium-111-radiolabel for plasmid DNA and its application to tissue distribution study. *Bioconjugate Chem* 2003; **14**: 955–961.
20. Liu F, Song Y, Liu D. Hydrodynamics-based transfection in animals by systemic administration of plasmid DNA. *Gene Ther* 1999; **6**: 1258–1266.
21. Tan Y, Li S, Pitt BR, *et al.* The inhibitory role of CpG immunostimulatory motifs in cationic lipid vector-mediated transgene expression in vivo. *Hum Gene Ther* 1999; **10**: 2153–2161.
22. Unlap M, Jope RS. Dexamethasone attenuates NF-κB binding activity without inducing IκB level in rat brain in vivo. *Mol Brain Res* 1997; **45**: 83–89.
23. Zhou D, Brown SA, Yu T, *et al.* High dose of ionizing radiation induced tissue-specific activation of nuclear factor-κB in vivo. *Radiat Res* 1999; **151**: 703–709.
24. Tripp CA, Wolf SF, Unanue ER. Interleukin 12 and tumor necrosis factor α are costimulators of interferon γ production by natural killer cells in severe combined immunodeficiency mice with listeriosis, and interleukin 10 is a physiologic antagonist. *Proc Natl Acad Sci U S A* 1993; **90**: 3725–3729.
25. Liu Y, Mounkes LC, Liggitt HD, *et al.* Factors influencing the efficiency of cationic liposome-mediated intravenous gene delivery. *Nat Biotechnol* 1997; **15**: 167–173.
26. Mahato RI, Kawabata K, Nomura T, *et al.* Physicochemical and pharmacokinetic characteristics of plasmid DNA/cationic liposome complexes. *J Pharm Sci* 1995; **84**: 1267–1271.
27. Nishikawa M, Huang L. Nonviral vectors in the new millennium: delivery barriers in gene transfer. *Hum Gene Ther* 2001; **12**: 861–870.
28. Templeton NS, Lasic DD, Frederik PM, *et al.* Improved DNA : liposome complexes for increased systemic delivery and gene expression. *Nat Biotechnol* 1997; **15**: 167–173.
29. Ren T, Song YK, Zhang G, *et al.* Structural basis of DOTMA for its high intravenous transfection activity in mouse. *Gene Ther* 2000; **7**: 764–768.
30. Ohno M, Fornerod M, Mattaj IW. Nucleocytoplasmic transport: the last 200 nanometers. *Cell* 1998; **92**: 327–336.
31. Dean DA. Import of plasmid DNA into the nucleus is sequence specific. *Exp Cell Res* 1997; **230**: 293–301.
32. Dean DA, Dean BS, Muller S, *et al.* Sequence requirements for plasmid nuclear import. *Exp Cell Res* 1999; **253**: 713–722.
33. Assogba BD, Choi BH, Rho HM. Transcriptional activation of the promoter of human cytomegalovirus immediate early gene (CMV-IE) by the hepatitis B viral X protein (HBx) through the NF-κB site. *Virus Res* 2002; **84**: 171–179.
34. Mesika A, Grigoreva I, Zohar M, *et al.* A regulated, NFκB-assisted import of plasmid DNA into mammalian cell nuclei. *Mol Ther* 2001; **3**: 653–657.
35. Sakurai F, Nishioka T, Yamashita F, *et al.* Effects of erythrocytes and serum proteins on lung accumulation of lipoplexes containing cholesterol or DOPE as a helper lipid in the single-pass rat lung perfusion system. *Eur J Pharm Biopharm* 2001; **52**: 165–172.
36. Aramaki Y, Takano S, Tsuchiya S. Cationic liposomes induce macrophage apoptosis through mitochondrial pathway. *Arch Biochem Biophys* 2000; **392**: 245–250.
37. McLean JW, Fox EA, Baluk P, *et al.* Organ-specific endothelial cell uptake of cationic liposome–DNA complexes in mice. *Am J Physiol Heart Circ Physiol* 1997; **273**: H387–404.
38. Deshpande D, Blezinger P, Pillai R, *et al.* Target specific optimization of cationic lipid-based systems for pulmonary gene therapy. *Pharm Res* 1998; **15**: 1340–1347.
39. Pan RY, Xiao X, Chen SL, *et al.* Disease-inducible transgene expression from a recombinant adeno-associated virus vector in a rat arthritis model. *J Virol* 1999; **73**: 3410–3417.
40. Loser P, Jennings GS, Strauss M, *et al.* Reactivation of the previously silenced cytomegalovirus major immediate early promoter in the mouse liver: involvement of NFκB. *J Virol* 1998; **72**: 180–190.
41. Vereecque R, Saudemont A, Wickham TJ, *et al.* γ-Irradiation enhances transgene expression in leukemic cells. *Gene Ther* 2003; **10**: 227–233.
42. Almoftia MR, Harashimab H, Shinoharaa Y, *et al.* Cationic liposome-mediated gene delivery: Biophysical study and mechanism of internalization. *Arch Biochem Biophys* 2003; **410**: 246–253.
43. Xu Y, Szoka FC Jr. Mechanism of DNA release from cationic liposome/DNA complexes used in cell transfection. *Biochemistry* 1996; **35**: 5616–5623.
44. Zabner J, Fasbender AJ, Moninger T, *et al.* Cellular and molecular barriers to gene transfer by a cationic lipid. *J Biol Chem* 1995; **270**: 18 997–19 007.
45. Shi F, Wasungu L, Nomden A, *et al.* Interference of poly(ethylene glycol)–lipid analogues with cationic-lipid-mediated delivery of oligonucleotides; role of lipid exchangeability and non-lamellar transitions. *Biochem J* 2002; **366**: 333–341.
46. Tan Y, Zhang JS, Huang L. Codelivery of NF-κB decoy-related oligodeoxynucleotide improves LPD-mediated systemic gene transfer. *Mol Ther* 2002; **6**: 804–812.

ELSEVIER

Available online at www.sciencedirect.com
ScienceDirect

Journal of Controlled Release 116 (2006) 90–95

journal of controlled release

www.elsevier.com/locate/jconrel

Suppression of tumor growth by intratumoral injection of short hairpin RNA-expressing plasmid DNA targeting β-catenin or hypoxia-inducible factor 1α

Yuki Takahashi, Makiya Nishikawa, Yoshinobu Takakura *

Graduate School of Pharmaceutical Sciences, Kyoto University, Kyoto, Japan
Department of Biopharmaceutics and Drug Metabolism, Graduate School of Pharmaceutical Sciences, Kyoto University, Sakyo-ku, Kyoto, 606-8501, Japan

Received 25 July 2006; accepted 8 September 2006
Available online 16 September 2006

Abstract

To inhibit the growth of murine melanoma B16 cells in mice, we downregulated the gene expression of β-catenin and hypoxia-inducible factor 1α (HIF1α) in the tumor cells by delivering short hairpin RNA (shRNA)-expressing plasmid DNA (pDNA) targeting one of these genes. Transfection of any of the shRNA-expressing pDNAs to B16 cells resulted in the reduction of the corresponding mRNA, which was associated with a reduced number of viable cells. A flow cytometric analysis of annexin V labeling assay was also performed to count the number of apoptotic cells. A flow cytometric analysis showed that the suppression of the expression of β-catenin or HIF1α in B16 cells increased the number of apoptotic cells. An intratumoral injection of pshβ-catenin (shRNA-expressing pDNA targeting β-catenin) or pshHIF1α (shRNA-expressing pDNA targeting HIF1α) followed by electroporation greatly suppressed the expression of the corresponding target mRNA in the intradermal tumor tissue. The growth of the intradermal tumor was significantly ($P<0.05$) suppressed by the treatment. In conclusion, tumor growth was successfully inhibited by the intratumoral delivery of pshβ-catenin or pshHIF1α.

Keywords: RNAi; Gene delivery; In vivo; Primary tumor; Electroporation

1. Introduction

Tumor cells are characterized by changes in the profile of protein expression. Such changes may lead to the imbalanced production of proteins relating to the malignancy of the cells, or to the production of mutated proteins with abnormal functions. The altered protein expression in tumor cells may contribute to the cell survival, unregulated proliferation and metastatic nature of the cells. Therefore, silencing the expression of these proteins in tumor cells can be a potent and target-specific cancer treatment with a low risk of side effects. RNA interference (RNAi) is a potent and ubiquitous gene silencing mechanism that downregulates the expression of a specific gene of interest [1–5]. After the discovery that short double-stranded RNA (siRNA) can induce RNAi in mammalian cells without stimulating interferon response [6,7], siRNAs have proven to be effective agents for suppressing specific gene expression. The early successes of induction of RNAi in cultured cells have led to high expectations for in vivo and therapeutic applications of siRNAs [8,9]. Cancer is one of the most important target diseases for RNAi-based treatment [10,11]. Contrary to conventional strategies, such as the use of antisense oligonucleotides which have been hampered by low potency and insufficient specificity, the use of siRNAs is reported to be more efficient and to have greater in vivo potency [12–15]. Therefore, RNAi-based gene silencing is a promising approach to achieve target-specific anticancer treatments.

Delivery of siRNA to tumor cells is the greatest obstacle to establishing RNAi as a therapeutic approach to treat cancer because the gene silencing effect is limited to cells that have received siRNA [16–18]. This is a major reason why few papers have reported the successful suppression of in vivo tumor growth by RNAi. In a previous study, we have investigated the

* Corresponding author. Tel.: +81 75 753 4615; fax: +81 75 753 4614.
E-mail address: takakura@pharm.kyoto-u.ac.jp (Y. Takakura).

0168-3659/$ - see front matter © 2006 Elsevier B.V. All rights reserved.
doi:10.1016/j.jconrel.2006.09.002

delivery of siRNA or short hairpin RNA (shRNA)-expressing plasmid DNA (pDNA) to tumor cells in mice [19]. We succeeded in effectively suppressing target gene expression in tumor cells by intratumoral injection of siRNA or shRNA-expressing pDNA followed by electroporation. Using melanoma cells stably expressing firefly luciferase, we found that a single intratumoral injection of shRNA-expressing pDNA following electroporation inhibits the expression by 30%. These results suggest that the delivery of shRNA-expressing pDNA can inhibit the tumor growth if a proper target gene in tumor cells is downregulated by this technique.

In addition to the delivery methods of siRNA, selection of target genes is an important issue that determines the RNAi effects on tumor growth. Although many genes encoding products that play important roles in tumor progression can be targets for RNAi-based suppression of tumor growth, we selected β-catenin and hypoxia-inducible factor 1α (HIF1α) genes as possible target genes to realize RNAi-based cancer therapy. β-catenin plays a key role in cell adhesion and also regulates the activity of certain transcription factors, T cell factor/lymphoid enhancer factor (TCF/LEF) in the Wnt pathway, which activates the transcription of genes related to cell growth and survival [20]. When injected intraperitoneally, siRNA targeting β-catenin complexed with Oligofectamine suppressed the proliferation of colon cancer HCT116 cells in the peritoneal cavity [21]. On the other hand, HIF1 is a heterodimer that consists of constitutively expressed HIF1β and HIF1α, and the expression of the latter is tightly regulated by oxygen concentration. HIF1 activates the transcription of genes that are involved in cancer biology, including angiogenesis, cell survival, glucose metabolism and invasion [22]. Sun et al. reported that intratumoral administration of pDNA which expresses antisense HIF1 suppressed the growth of tumor tissue [23]. In addition, HIF1 was evaluated as a cancer therapeutic target via inducible RNA interference in vivo [24].

Therefore, suppressing the expression of these target genes is expected to inhibit tumor growth. To suppress the expression of these target genes, we constructed and used shRNA-expressing pDNA, not siRNA, to induce RNAi in tumor cells, because (i) shRNA-expressing pDNA shows more sustained RNAi effects than siRNA, and (ii) there was little difference in the delivery efficiency to tumor cells between shRNA-expressing pDNA and siRNA. We report here that shRNA-expressing pDNA targeting β-catenin or HIF1α effectively suppresses tumor growth in mice following intratumoral injection followed by electroporation.

2. Materials and methods

2.1. shRNA-expressing pDNA

shRNA-expressing pDNAs driven by human U6 promoter were constructed from piGENE-hU6 vector (iGENE Therapeutics, Tsukuba, Japan) according to the manufacturer's instructions. Target sites in murine genes encoding β-catenin and HIF1α were as follows: β-catenin site1, 5′-GCGGTAGGG TAAATCAGTA-3′, site2, 5′-GAATGAGACTGCAGATCTT-3′; HIF1α site1, 5′-GTGAAAGGATTCATATCTA-3′, site2, 5′-GACACAGCCTCGATATGAA-3′. These pDNAs transcribe a stem-loop-type RNA with loop sequences of ACG UGU GCU GUC CGU. piGENE-hU6 vector, which transcribes a non-related sequence of RNA with partial duplex formation, was used as a control pDNA throughout the present study. Each pDNA was amplified in the DH5α strain of *Escherichia coli* and purified using a QIAGEN Endofree Plasmid Giga Kit (QIAGEN GmbH, Hilden, Germany).

2.2. Cell culture

A murine melanoma cell line B16-F1, B16-BL6 and B16-BL6 cells that stably express firefly luciferase and sea pansy luciferase (B16-BL6/dual Luc) were cultured in Dulbecco's modified Eagle's minimum essential medium (DMEM; Nissui Pharmaceutical, Tokyo, Japan) supplemented with 10% fetal bovine serum (FBS) and penicillin/streptomycin/L-glutamine (PSG) at 37 °C and 5% CO_2/95% air [19].

2.3. In vitro transfection

B16 cells were plated on culture plates. After an overnight incubation in DMEM containing 10% FBS and PSG at 37 °C in 5% CO_2/95% air, transfection of pDNA was performed using Lipofectamine 2000 (Invitrogen, Carlsbad, CA, USA) according to the manufacturer's instructions. In brief, 1 μg pDNA was mixed with 3 μg Lipofectamine 2000 at a final concentration of 2 μg pDNA/ml dissolved in OPTI-MEM I (Invitrogen), and the resulting complex was added to the cells and the cells were incubated with the complex for 4 h. Cells were washed with PBS and further incubated with the culture medium as described above for specified time periods up to 96 h.

2.4. mRNA quantification

Total RNA was isolated using MagExtractor MFX-2100 and a MagExtractor RNA kit (TOYOBO, Osaka, Japan) following the manufacturer's protocol. To eliminate DNA contamination, the total RNA was treated with DNase I (Takara Bio, Otsu, Japan) prior to reverse transcription. Reverse transcription was performed using a SuperScript II (Invitrogen) and dT-primer following the manufacturer's protocol. For quantitative mRNA expression analysis, real-time PCR was carried out with total cDNA using a LightCycler instrument (Roche Diagnostics, Basle, Switzerland). The sequences of the primers used for amplification were as follows: GAPDH forward, 5′-CTGCCA AGTATGATGACATCAAGAA-3′, reverse, 5′-ACCAGGAAA TGAGCTTGACA-3′; β-catenin forward, 5′-CCTGCAGAAC TCCAGAAAG-3′, reverse, 5′-GTGGCAAAAACATCAAC GTG-3′; HIF1α forward, 5′-TCAAGTCAGCAACGTGGA AG-3′, reverse, 5′-TATCGAGGCTGTGTCGACTG-3′. Amplified products were detected on-line via intercalation of the fluorescent dye SYBR green (LightCycler-FastStart DNA Master SYBR Green I kit, Roche Diagnostics). The cycling conditions were as follows: initial enzyme activation at 95 °C for 10 min, followed by 55 cycles at 95 °C for 10 s, 60 °C for 5 s, and 72 °C for 20 s. Gene-specific fluorescence was measured at